1982

Strength of rectangular composite box girders: testing of large size composite box girders

Ben T. Yen

Y. S. Chen

Lehigh University

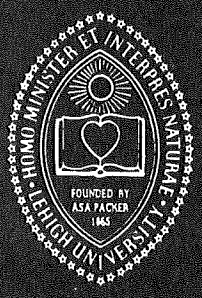

Fritz Engineering Laboratory

Strength of Rectangular Composite Box Girders

TESTING OF LARGE SIZE COMPOSITE BOX GIRDERS

by

B. T. Yen

Y. S. Chen

Report No. 380.11

Technical Report Documentation Page

1. Report No.	2. Government Accession No.	3. Recipient's Catalog No.
FHWA/PA 82-010		

4. Title and Subtitle	5. Report Date
Testing of Large Size Composite Box Girders	April 30, 1982
	6. Performing Organization Code
7. Author(s)	8. Performing Organization Report No.
B. T. Yen and Y. S. Chen	Fritz Engineering Laboratory Report No. 380.11
9. Performing Organization Name and Address	10. Work Unit No. (TRAIS)
Fritz Engineering Laboratory #13 Lehigh University Bethlehem, Pennsylvania 18015	11. Contract or Grant No. 69-4
	13. Type of Report and Period Covered
12. Sponsoring Agency Name and Address	Interim Report
Commonwealth of Pennsylvania Department of Transportation	14. Sponsoring Agency Code

15. Supplementary Notes

Prepared in cooperation with the United States Department of Transportation, Federal Highway Administration, from the study "Strength of Rectangular Composite Box Girders"

16. Abstract

Two "large size" composite box girder specimens were tested. Each was subjected to a series of preliminary loading before testing to failure under combined bending moment and torsion. This report summarizes briefly the results of testing, with emphasis placed on behavior and mode of failure of the composite box girders.

The slender webs of composite box girders behaved similar to webs of simple plate girders: post-buckling, diagonal, tension fields developed under relatively high shear. When the web buckling strength was high, yielding of steel tension flange or buckling of steel compression flange took place first. The failure of a composite box girder occurred when, at least, both flanges and a web or both webs and a flange have failed.

17. Key Words	18. Distribution Statement
Bending moment, Box Girder, Buckling, Concrete Deck, Composite, Failure, Flange, Steel, Tension Field, Tests, Torsion, Web	

19. Security Classif. (of this report)	20. Security Classif. (of this page)	21. No. of Pages	22. Price
Unclassified	Unclassified	95	

COMMONWEALTH OF PENNSYLVANIA

Department of Transportation

Research Division
Office of Research and Special Studies

Wade L. Gramling, P.E. - Chief Research Engineer

Project 69-4: Strength of Rectangular Composite Box Girders

TESTING OF LARGE SIZE COMPOSITE BOX GIRDERS

by

B. T. Yen

Y. S. Chen

Prepared in cooperation with the Pennsylvania Department of Transportation and the U. S. Department of Transportation, Federal Highway Administration.

Lehigh University

Office of Research

Bethlehem, Pennsylvania

April 1982

Fritz Engineering Laboratory Report No. 380.11(82)

TABLE OF CONTENTS

1. INTRODUCTION

The behavior of box girders in the elastic range of material properties has been studied extensively.[1.1, 1.2, 1.3] In the United States of America box girders with a U-shaped or trapezoidal-shaped steel section and a concrete deck are much more common than those with a closed steel cross section. The sizes of the composite box girders are such that the deck width usually constitutes the full width of the roadway or a traffic lane of highway bridges. The span length commonly is below 150 ft. In analysis, the concrete deck is converted to an equivalent steel plate and traditional procedure of stress evaluation is employed assuming no buckling of plates will occur.

Because the webs of composite box girders are similar to the webs of plate girders, their behavior under load could be expected to be also similar. For plate girders, postbuckling tension field action of web panels contributes to the load carrying capacity.[1.4, 1.5] Therefore, postbuckling strength of webs in composite box girders could also contribute to their load-carrying capacity. The primary difference between plate girders and composite box girders is that the box girders are anticipated to resist torsional loads in addition to flexure loads. Consequently, the two webs of a composite box girder usually are not subjected to equal forces.

Composite box girders also differ from very large steel box girders, which consist of large stiffened plates for the four sides

of the box shape. For these stiffened plates, the postbuckling behavior of a single plate panel is of minor significance as compared to the buckling strength of the stiffened plate as a whole. The strength behavior of large steel box girders, therefore, would be different from that of composite box girders.[1.6, 1.7]

While analytical studies for stress evaluation of composite box girders were being made,[1.8] testing of relatively "large size" models of such members were conducted. These models were regarded as large in that the effects of residual stresses from welding, of out-of-flatness of steel plates, and of interaction between the steel portion and the concrete deck were all inherent in the specimens. The results of these tests provided information for the development of a procedure for the evaluation of composite box girder load carrying capacity.[1.9, 1.10]

This report summarizes briefly the results of testing these two relatively large-sized composite box girders. Emphasis is placed on the behavior and mode of failure of the composite box girders.

2. SPECIMENS AND LOADING

2.1 Specimens

Two "large size" composite box girder specimens were fabricated for testing. The elevation and cross-section of the specimens are sketched in Figs. 2.1 and 2.2.

These specimens, designated as L1 and L2, had an overall length of 40'-10". The steel portion of each box girder was U-shaped, 41 in. high and 40 in. wide. A 4 in. thick concrete deck, with two layers of No. 4 reinforcing bars at 6 in. center-to-center in both directions, is connected to the steel portion by 1/2 in. stud shear connectors along the top flanges of the U-shape and the top flange of the diaphragms. The shear connectors in pairs at 7 in. spacing, were arranged to ensure complete interaction between the concrete and the steel portions.[2.1, 2.2]

Specimen L1 was proportioned according to contemporary allowable stress approach, and Specimen L2 to the load factor design provision. The result was that Specimen L1 had 1/4 in. web plates, fairly close spacing of web transverse stiffeners (aspect ratio 0.75), and two longitudinal stiffeners for the bottom flange. Specimen L2 had 3/16 in. webs, web stiffener spacing equal to or greater than the web depth (aspect ratio 1.0 to 1.5), and only one bottom flange longitudinal stiffener. The nominal dimensions of the component parts are summarized in Table 2.1.

The steel flanges and webs were made of ASTM A36 plates. The tensile properties of the steel components and the compressive properties of the deck concrete were obtained through standard tests as specified by ASTM. These results, as well as some other mechanical properties of the steel and concrete, are given in Table 2.2.

From the girder dimensions and material properties, the cross sectional characteristics of the composite box girders could be calculated according to the procedure of Reference 1.8. For these two test girders, the shear lag effect was small, and the contribution of the reinforcing bars was also small. The cross sectional properties, therefore, were evaluated using the traditional method of thin-walled elastic beams.[2.3, 2.4] The results are listed in Table 2.3.

2.2 Setup and Loads

The test specimens were setup for testing according to the intended loading conditions. Each specimen was subjected to a series of preliminary static loading before construction of the concrete deck. These include open U-shaped steel portions under torsion plus positive and negative bending moment, separately, and braced steel U-shape portions under similar loading. Repeated (cyclic) loads were then applied to each composite box girder inducing bending moment and torsion.

For the load carrying capacity tests of the composite box girders, testing was conducted in the 5,000,000 pound capacity testing machine. Figure 2.3 shows the setup for negative bending moment and torsion. The load was applied at the far (east) end of the specimen,

directly over the north web. The roller support was 10 ft. west of the load, and the west end of the composite box girder was tied down so as to prevent lifting from the support. The schematic sketch of this setup, as well as that for positive bending moment and torsion, are given as Fig. 2.4. For easy identification, the west and east supports were designated as points A and C, respectively, whereas the load points for positive bending and negative bending were assigned B and D, respectively. The composite box girder in Fig. 2.3 is Specimen L1, thus the setup was for L1-CD. Figure 2.5 shows the setup after the test L1-CB, (L1, composite, load at point B). The idle, overhanging east end of test L1-CB is shown in Fig. 2.6.

The test sequence and the corresponding test loads are listed in Table 2.4. The magnitudes of loads for the preliminary tests were determined from analysis in order to ensure elastic behavior of the specimens.

For the repeated loading (fatigue testing), the composite box girders were subjected to constant bending moment and alternating torsional loads. The setup for test L1-FB is shown in Fig. 2.7, looking from west end towards east. The downward loading jack over the south (right) web exerted constant force, while the upward loading jack directly below was coupled to the third jack. These coupled jacks induced repeated torsion to the composite box girder.

3. PRELIMINARY TESTS

The preliminary tests were for the purpose of generating some data to confirm the analytical procedure. Confirmation was made through comparison of measured and computed stresses and deflections.[1.8] So far as the stresses were kept within the elastic limit, the computed and measured values correlated fairly well. For example, the load-deflection plots in Figs. 3.1 and 3.2 for the open U-shaped L1 show that the computed vertical deflection (thin lines) at the bottom flange were close to the measured values (dots). The specimen returned practically to its original state when the applied loads were removed. It was rather "uneventful" for all the preliminary tests. To summarize these tests, the load-deflection results are given as Figs. 3.1 to 3.8.

Figures 3.1 and 3.2 are for Specimen L1, open U-shape, which was not strong in resisting torsional loads. For both positive and negative bending moment cases, L1-OB and L1-OD, the north web to bottom flange junction deflected more than the corresponding point on the south side. This was also the condition for L2, as shown in Figs. 3.3 and 3.4. Specimen L2 had slightly thinner webs and larger spacing between web stiffeners, thus had slightly larger deflection magnitudes than Specimen L1. The linear elastic behavior of the specimens is evident from the linear load-deflection relationship.

The bracing members at the top flange level rendered the specimens stronger in resisting torsional loads. Diagonal bracing members were used, with the configuration sketched in Figs. 3.5 to 3.8. In analysis, these bracing systems could be converted into equivalent plates to form equivalent closed box girders for estimation of stresses and deflections.[3.1, 3.2] Again, as long as the applied loads did not cause yielding or large deformation of box girder cross-sections, estimated and measured stresses and deflections correlated fairly well.[3.2]

Comparison of corresponding deflections for the open and braced U-shapes reveals the effectiveness of the top bracing system. Figure 3.9 combines Figs. 3.1 and 3.6, showing the deflections of Specimen L1 under positive bending moment and torsion. With top flange bracing, the difference between deflections under the north (loading) and south web decreased. The bracing system also increased the yield strength, Py, the magnitude of applied load which caused first yielding at a single point in the specimen. Similar results occurred to the other loading cases.

The fatigue loading applied to the composite box girders was for examining possible damages due to repeated torsional loads. The test setup for L1-FB is shown as Fig. 2.7. Figure 3.10 is a schematic of the loads, showing the induced bending moment and torsion. The resulting bending moment was constant while the torsion fluctuated between clockwise and counterclockwise directions. The concrete deck was under compression and shearing stresses. For composite box girder

L2, the loads were applied at the overhang. Therefore, the concrete deck was under tension and shear.

There was no fatigue damage detected in the concrete deck of either composite box girder. During repeated loading of L2-FD, transverse hair cracks in the concrete deck could be observed to undergo very slight opening-and-closing behavior, but the cracks did not propagate. These transverse hair cracks existed before any application of load and were probably shrinkage cracks exaggerated during setting up of the box girder onto the testing position.

No fatigue damage to the steel portion was expected. The applied stress ranges at various steel structural details, such as ends of stiffeners and stud shear connectors, were all well below the specified allowable values.(2.1).

4. TESTS IN POSITIVE BENDING MOMENT AND TORSION

4.1 Failure by Flanges

For a composite box girder subjected to positive bending moment and torsion, the concrete deck is in compression, the steel bottom flange is in non-uniform tension, and the two webs are under different magnitude of bending and shear.[1.8] If the webs are sufficiently strong to carry bending and shear, the tension flanges will reach yielding first. Thereafter, deflection of the composite box girder would increase at a higher rate. Failure of the specimen would occur when the top flange has also reached its capacity.[4.1, 4.2]

Composite box girder test L1-CB under-went such a failure mode as described above. The web buckling strength was much above the bottom flange yield load. At about 420 kips, the flange reached general yielding, as is indicated by the load-strain plots of Fig. 4.1. As applied load increased, box girder deflection increased faster. This is depicted in the load-deflection curves of Fig. 4.2. The stress distribution in a cross-section a short distance away from the load point, Fig. 4.3, showed that yielding penetrated up the bottom of the webs. At about 520 kips, concrete adjacent to the load point started to be crushed. At 550 kips the concrete deck broke and the north web near the load point developed tension-field troughs. The composite box girder had three of its four sides of a cross-section failed, and the box girder reached its ultimate strength.

The general appearance of the failed area after testing is shown in Fig. 4.4. The crushed concrete deck, the typical tension field yield lines in the web,[4.3] and the permanent deflected curve of the bottom flange can all be seen.

Figure 4.5 is a closeup photograph showing the failed deck and the nodal lines on the web surface. The bottom portion of the deck failed in tension due to bending of the deck. About 2 ft. away, the average deck strain was reduced after the deck failure. The load-strain relationship of the deck at Z = 225 in. is depicted in Fig. 4.6.

The load-deflection curves of test L1-CB has the general characteristics of a typical steel-concrete composite beam.[2.2, 4.4] The curves have two generally linear portions: the steep portion corresponds to elastic behavior and the flat portion to the penetration of yielding of the web(s). Failure of the concrete flange triggers the failure of the specimen.

4.2 Failure by Web and Flanges

For composite box girders under positive bending moment and torsion, if web buckling strength is lower than the bottom flange yield load, post-buckling tension field action of the web will develop.[4.5] The steel bottom flange and the concrete deck both must resist component forces from the diagonal tension field. When both flanges fail, the box girder has three of its four sides failed and its ultimate strength is then reached.

Composite box girder L2 had relatively slender webs with transverse stiffeners spaced fairly far apart (Fig. 2.1). The web buckling strength was lower than the flange yielding strength. When 300 kips were applied at middle of the span (Fig. 2.4, Test CB), some panels of the north web developed tension field action. At 410 kips tension field action was prominent in many of the web panels. The deflection of the composite box girder, however, remained small. The load-deflection plots are almost straight, as it is depicted in Fig. 4.7. When higher loads were applied, the concrete deck and the steel bottom flange as well as the upper portion of the bearing stiffeners at west end started to show signs of failure. Girder deflection increased at a higher rate. At 462 kips, both flanges at this box panel failed, and the composite box girder could not take any additional loads.

The failed end panel of the north web is shown in Fig. 4.8. The diagonal tension field was signified by the dark band in the web. The concrete deck was pulled down, causing a large crack, and the steel bottom flange was pulled up. Figure 4.9 shows the "kink" at the bottom flange and the general appearance of the composite box girder. The telltale diagonal mark of tension field can be seen in every panel. This is more obvious in Fig. 4.10. On the other side of the composite box girder, in the south web, tension field action also took place. Figure 4.11 shows the deflected web and transverse stiffener at Z = 115 in. of the south web.

By examining Fig. 4.8 carefully, it can be seen that the upper portion of the bearing stiffeners were bent. This is clearly shown in Fig. 4.12, a photograph taken after removal of testing apparatus. Figure 4.13 records the yield lines on the surface of the bearing stiffener at the end of the box girder. This type of failure condition is typical of end panels of plate girders when tension field action developed in the end panel. For test L2-CB, the second panel from the west end had a longer panel length with an aspect ratio of 1.2, thus developed tension field action earliest. However, because the flanges were not subjected to high stresses, failure did not take place in this panel. It was the inability of the end bearing stiffeners to resist the tension field components that lead to the failure of the concrete deck.

Although tension field action occurred in every panel, the flange strains were nominal all along the box girder. Figure 4.14 and 4.15 show the measured strains at cross-section Z = 212.5, not far from the load point. The steel bottom flange never reached yielding, as it is seen in Fig. 4.14. The concrete adjacent to the load point was crushed locally (see Fig. 4.15) but obviously did not cause a problem.

The load deflection curve of L2-CB in Fig. 4.7 also has the general characteristics of a steel-concrete composite beam, as described earlier.

The conclusions from these composite box girder tests in positive bending moment and torsion is that the ultimate strength of

the box girder is reached when both flanges have failed with failure of at least one of the webs.

5. TESTING IN NEGATIVE BENDING MOMENT AND TORSION

5.1 Failure by Compression Flange

A composite box girder under negative bending moment and torsion subjects the steel bottom flange to compression and shear. If the webs are sufficiently strong to carry bending and shear, and the concrete deck does not fail, then the buckling strength of the steel bottom flange controls the load carrying capacity of the composite box girder.

Composite box girder test L1-CD failed by compression flange buckling. The test setup is shown in Figs. 2.3 and 2.4. The load at the end of the overhanging portion induced relatively high shear plus bending moment in the web and compressive forces and shear in the bottom flange. Since the web stiffeners were spaced to prevent web buckling, the steel compression flange would fail first. Figure 5.1 shows the bending moment and torsion diagram for the box girder. The highest bending moment, thus the highest compression in the steel flange, was near the interior support C. Failure would occur between B and C because of the moment gradient.

The failed steel bottom flange of Test L1-CD is shown in Fig. 5.2. The photograph shows an inclined view from below the flange. It was located in the second panel from the support C, and was in panel 11 of Fig. 5.1. As the flange buckled (deflected) gradually with the increasing magnitude of the applied load, the deflection of the

steel flange plate caused bending of the webs. The partially failed south web of the panel is shown in Figs. 5.3 and 5.4. The composite box girder had one side of a panel failed, a second side started to fail, but the box girder had not reached its load carrying capacity. In order to preserve the composite box girder for other tests, (that is, Test L1-CB), the applied load was removed.

At the suspension of testing, part of the steel bottom flange had reached yielding. The diagram of load versus stress (or strain times Young's modulus) in Fig. 5.5 shows that the bottom flange yielded directly under the south web, the web shown in Figs. 5.3 and 5.4. The corresponding load-deflection diagrams of the box girder are plotted as Fig. 5.6. After the applied load was removed, there was little permanent deflection of the box girder as a whole, but there was permanent deflection of the bottom flange at the "buckled" location.

When test L1-CD resumed after testing the single span portion in positive bending and torsion, the box girder sustained a maximum load of 282.5 kips. Failure again was initiated by buckling of the steel bottom flange. Figure 5.7 shows the profile of the bottom compression flange at location of failure. (The whitewash had been brushed away).

The failure was in the first panel from the support, panel 12 (see Fig. 5.1). The compression flange deflected (buckled) gradually as load was increased. The deflection caused the webs to bend. Yielding of the web-to-flange junctions then took place. The webs subsequently failed. The component parts of the box girder panel was

not able to carry additional loads and the ultimate strength of the box girder was reached.

The appearance of the south web and north web after testing are shown in Figs. 5.8 and 5.9, respectively. The failed web panel in Fig. 5.9 is the first to the right of three bearing stiffeners. The locally deflected steel compression flange can be seen clearly. This failure mode was analogous to that of Fig. 4.4 (with the concrete compression flange on top), and is typical of steel plate girders.[4.3]

The concrete deck was the tension flange of the composite box girder under negative bending moment. Small cracks transverse to the length of the deck existed when the box girder was under its own weight in the testing position. When the magnitude of the applied load increased, these cracks widened and grew deeper. The widened cracks concentrated primarily over the region of the interior support. Under higher and higher loads, these cracks spread toward the loading end and the centerline of the anchoring span, while diagonal cracks started to appear near the support C. More and more diagonal cracks formed closer and closer to the load point as the applied load got higher and higher. Figure 5.10 shows a bird's eyeview of the crack pattern on the surface of the concrete deck of the overhanging portion. The cracks were marked by black ink and the magnitudes of the applied load were also indicated. The load point is at the lower righthand corner; those two holes for lifting cables were directly over support C.

No attempt was made to examine the concrete crack depth. For practical purpose, an effective deck thickness was considered for analysis. It was found from this and other tests[1.8] that a partial deck thickness equal to the distance between the bottom of the deck and the center of the bottom layer longitudinal reinforcing steel bars, could provide satisfactory comparison of stresses and deflections in the linear elastic stage of composite box girder behavior. An example of comparison is given as Fig. 5.11, in which the box girder deflection of Test L1-CD is fairly well estimated by the partial deck thickness assumption.

Another concern of composite box girder in negative moment and torsion was the possibility of sudden buckling of the steel compression flange. This phenomenon did not occur in Test L1-CD, nor during the similar test of composite box girder L2. Strain measurements revealed that the steel flange plate deflected gradually, with a change of rate prior to and after flange failure. The recorded strains at the center of bottom flange 315 in. from the west support are shown in Fig. 5.12. The location was where flange failure took place before the suspension of testing. At this location, the increase of compressive strains in the flange plate was slightly higher inside the box than outside. The difference in magnitude of strains indicated the amount of local bending or deflection of the steel flange. The difference increased with the magnitude of the applied load. The change of rate between 200 kips and 236.5 kips could not be considered as an indication of flange failure. The change of rate

was actually much higher after 260 kips when failure occurred at the flange plate nearby, in panel 12 next to support C.

Strain distribution in cross-sections of composite box girders also can only be used to record changes which had taken place, not to predict failure of the steel compression flange. The distribution of longitudinal strains in two cross-sections are shown in Figs. 5.13 and 5.14. Cross-section Z = 315 in. in Fig. 5.13 is at the center of panel 11 (see Fig. 5.1). At lower loads, such as 100 kips here, the distribution of mean strain in the steel plates were linear. At 200 kips, the slight deviation from linear distribution was an indication of deflection of the flange and the web plates. The condition of the web plate strains is typical of plate girders.[4.3] At 236.5 kips, when testing was temporarily suspended the strain distribution did not differ much from that for lower loads. Only at the maximum load of the box girder, at 282.5 kips, did the pattern of strain distribution change to a large degree.

The same general condition of strain distribution occurred at cross-section Z = 377.5, shown in Fig. 5.14. The cross-section was in the overhanging span, about one and a half feet from the support. At the maximum load of 282.5 kips, although failure happened at the other side of the support, the north web of this panel was well into tension field action. (See the diagonal yield band in the panel next to the bearing stiffeners of Fig. 5.9.) The change of strain distribution pattern testifies to this development of tension field. The recorded strains on the inside and outside surface of the north

web, shown in Fig. 5.15, reveal more on the behavior of the web at this location.

5.2 Failure by Webs and Compression Flange

When the buckling strength of the steel webs is lower than that of the steel bottom flange in compression, postbuckling tension fields develop under shearing forces. Failure of the composite box girder in negative bending moment and torsion occurs when the compression flange also fails. Composite box girder test L2-CD had this mode of failure.

Failure was in panel 8 (see Fig. 5.1), the first panel of the overhanging portion of the composite box girder. The appearance of the failed webs and bottom flange after testing are shown in Figs. 5.16 to 5.19. Figure 5.16 shows that the north web of this panel developed a diagonal tension field and the flange failure caused the tension field troughs to bend toward the flange buckle. A closeup photograph of the buckled flange at the end of the curved trough is shown in Fig. 5.17. The flange buckle spread over a length of about three feet from the support. The buckled, very wavy compression flange after completion of testing is shown in Fig. 5.18. At the south web next to the support the flange buckled, tension field yield band developed, and local yielding occurred directly above the support. These can be seen in Fig. 5.19.

It must be pointed out that the appearance of the failed panel, as shown in Figs. 5.16 to 5.19, was prominent because the

overhanging portion of the composite box girder was subjected to additional deflections (50%) beyond those at the maximum load. The load versus end deflection diagrams for Test L2-CD are plotted in Fig. 5.20. These type of load deflection diagrams are typical of welded plate girders with slender webs and normal size compression flanges.[4.3]

While additional deflections were imposed on the composite box girder, the north web of the end panel near the load point incurred the typical tension field failure at end bearing stiffeners.[4.3] Figure 5.21 is an overall view of the web panel and Fig. 5.22 shows the yielded zone between the stiffeners and the slightly bent flange. Comparison of Figs. 5.21 and 5.22 with Figs. 4.8 and 4.12 reveals the similarity between the failure of the end panels. In the case of a steel flange, the resistance to the vertical component of the tension field force was relatively low; the flange bent. For the Test L2-CB the composite compression flange was fairly rigid against vertical pull; the end bearing plates were bent before the compression flange was cracked.

For Test L2-CD, the concrete deck was in tension. The existence of hair cracks before application of loads and the crack patterns during testing were similar to the conditions of Test L1-CD, described in Section 5.1. The transverse and diagonal cracks are shown in Figs. 5.23 and 5.24, two photographs taken after testing and removal of all loads.

During testing, at the maximum applied load (P = 199.5 kips) the measured strains in the failed box panel confirmed the buckling

of the north web and the bottom flange. The distribution of longitudinal direction stresses at cross-section at midpanel (Z = 392.5) is plotted in Fig. 5.25. The relatively low stresses at mid-depth of the north web and the corresponding nonlinear distribution of stresses in the web are indications of web buckling. For the bottom flange, although there was a longitudinal stiffener, buckling occurred and the compressive stress was reduced at the mid-width with corresponding increase of stresses at the flange-to-web junctions. By examining the stress distributions at lower loads, it can be seen that the bottom flange was capable of resisting compression at 180 kips and the north web had already buckled at 100 kips.

The development of strains in the longitudinal direction at the center of the failed north web panel, is depicted by Fig. 5.26. The outside surface was bending concavely thus had increasingly higher compression; the inside face convexly, tension. This condition and web deflection, or buckling, continued until just before the maximum load, when the compression flange also buckled. The average of these two stress diagrams is also plotted in Fig. 5.26. It has the same general trend as that for the outside surface.

The average longitudinal stresses in the bottom flange at the web junctions of the cross-section, Z = 392.5, are given in Fig. 5.27 as load-strain diagrams. The corresponding strains near the edge of the concrete deck are plotted in Fig. 5.28. The steel flange yielded toward the end of testing. The through-the-thickness stresses in the concrete deck was always low, except at the north side over the support.

There, the tensile stress increased very much when the composite box girder was near its load carrying capacity. This indicated that the deck (or part of the deck) was capable of resisting some tensile forces.

For both Test L1-CD and L2-CD, where composite box girder segments are subjected to negative bending moment and torsion, the load carrying capacity was controlled by the failure of the steel compression flange and the two webs.

6. SUMMARY AND CONCLUSIONS

Fatigue (cyclic) loading of two million cycles in repeated torsion did not cause damage to the composite box girders. The behavior of the composite box girders during testing to failure under bending moment and torsion is summarized as follows.

1. Within the range of elastic properties of the materials, and without buckling of steel plate components, the behavior of the composite box girders could be predicted through analysis for bending and torsional loads. There was no visual damage, nor was there any nonlinear characteristics from the measured strains and deflections.
2. When composite box girder L1 (proportioned according to allowable stress design) was under positive bending and torsion, the steel bottom flange was in nonuniform tension. The webs of the box girder were designed to withstand shear forces without buckling, and yielding of the tension flange was the first major deviation from elastic behavior. When yielding penetrated the web and progressed upward into the web, box girder deflection increased at a high rate. Failure of the box girder occurred when the concrete deck cracked under compression and bending and the web buckled nearby. At this state, three of the four sides of a box cross-section failed.

3. Composite box girder L2, proportioned according to load factor design, to utilize the postbuckling strength of the web, developed web buckling and tension field under positive bending moment and torsional load. Failure occurred at the end panel of the box girder where both the concrete deck and the steel bottom flange were pulled toward the web.
4. When composite box girder L1 was subjected to negative bending and torsion, the steel bottom flange was in compression and the concrete deck in tension. Buckling of the steel compression flange caused local bending and yielding of the web. At the maximum load, the webs in the panel of the buckled flange also buckled.
5. Composite box girder L2, with relatively low strength against web buckling, had many buckled web panels when the steel bottom flange failed at failure of the box girder under negative bending moment and torsion.
6. For all tests, the phenomenon of steel plate buckling was not a sudden occurrence. Rather, the web or flange plate deflected out of plane gradually with an increased rate as applied load was increased on a composite box girder.
7. Under negative bending moment and torsional load, the concrete decks had cracks in the diagonal as well as the transverse direction.

8. The load-deflection diagram of a composite box girder in positive bending moment and torsion was similar to that of a simple composite beam in bending. The load-deflection curve was bilinear.
9. For each web of the composite box girders, its behavior under load was very similar to that of steel plate girders.

From these observed phenomena of composite box girders undergoing tests to failure, the following conclusions can be drawn.

A. The component parts of composite box girders under bending moment and torsion behaved in accordance with the imposed forces on these components: the web plates in high shear could develop postbuckoing tension field, the steel flange in compression could buckle, and the concrete deck could crack under tension and crush under high compression.
B. The failure of a composite box girder occurred only when three or more of the four components of a box section failed, making the box section incapable of withstanding additional loads.
C. Although the stresses and deflections became nonlinear after yielding had initiated in a component part or after buckling had introduced large deflection of steel plates, the distribution of stresses in a cross-section did not change drastically, except for the yielded or buckled

portion. This condition permitted the assumption that the strength and failure mode of each component could be evaluated separately.

D. The relative strength of the component parts of a composite box girder dictated the failure mode and strength of the box girder according to the external loading.

These few tests provided insight to the behavior of composite box girders, as well as served as basis for the development of procedures for estimating the ultimate strength of composite box girders.

ACKNOWLEDGMENT

This investigation was part of the research project, "Strength of Rectangular Composite Box Girders", sponsored by Pennsylvania Department of Transportation (69-4) in conjunction with the Federal Highway Administration. The sponsorship is highly appreciated.

The tests were conducted in Fritz Engineering Laboratory and Department of Civil Engineering, Lehigh University.

The opinions, findings and conclusions expressed in this report are those of the authors and not necessarily those of the sponsors.

Thanks are due Mrs. Dorothy Fielding for handling and processing the report.

TABLE 2.1

COMPONENT DIMENSIONS OF SPECIMENS

	Allowable Stress L1	Load Factor L2
Concrete Deck	4" x 72" x 40'-10"	
Concrete Reinforcement	#4 @ 6" x 6", two layers	
Shear Connectors	Two 1/2"Ø x 4" at 7"	
Top Steel Flanges	5/8" x 9"	
Web	1/4" x 40"	3/16" x 40"
Bottom Flange	3/8" x 40"	
Web Bearing Stiffeners	Three 2-5/8" x 2"	
Web Intermediate Stiffeners	5/8" x 2"	
Bottom Flange Long. Stiffeners	Two 5/8" x 2-1/2"	One 5/8" x 2-1/2"
Plate Diaphragms	5/8" x 40" x 36"	
K-Diaphragm	---	Two ∠3" x 3" x 1/2"
Top Bracing	5/8" x 9"	5/8" x 9"
Web Slenderness Ratio	160	213
Web Panel Aspect Ratio	0.625 - 0.75	1.0 - 1.5

TABLE 2.2

MECHANICAL PROPERTIES OF SPECIMEN COMPONENTS

(All Stresses in ksi)

Comonents		Property	L1	L2
Steel	Top Flange	Yield Stress*	36.7	36.7
	Web		42.6	56.9
	Bottom Flange		38.0	37.6
	Top Flange	Tensile Stress*	69.4	69.4
	Web		72.7	75.0
	Bottom Flange		66.5	66.6
	Top Flange	Elongation (% of 8")	26.8	26.8
	Web		24.4	22.2
	Bottom Flange		23.8	28.7
		Young's Modulus	29,500	
		Shear Modulus	11,350	
		Poisson's Ratio	0.30	
Concrete		Compressive Strength*	5.50	4.21
		Young's Modulus	3980	3390
		Shear Modulus	1700	1450
		Poisson's Ratio	0.17	
Deck Reinforcement		Yield Stress*	48.0	

*Test Results

Table 2.3

SECTIONAL PROPERTIES OF COMPOSITE BOX GIRDER SPECIMENS

	Allowable Stress L1	Load Factor L2
Transformed Area of Cross Section ($in.^2$)	86.0	76.3
Distance from N.A. to mid-thickness of Bottom Flange (in.)	29.5	28.9
Moment of Inertia about Horizontal Axis, I_x ($in.^4$)	26,000	24,200
Moment of Inertia about Vertical Axis, I_y ($in.^4$)	29,700	25,800
Shear Center Above N.A. (in.)	1.44	1.37
St. Venant Torsional Constant K_T ($in.^4$)	19,600	16,600
Warping Moment of Inertia, I_ω ($in.^6$)	1.32×10^6	1.52×10^6
Central Moment of Inertia, I_c ($in.^4$)	28,100	26,100
Warping Shear Parameter μ	0.302	0.362

TABLE 2.4

TEST SEQUENCE AND LOADS

	Test	L1 (kips)	L2 (kips)
Open U	OB	120	90
	OD	90	60
Braced U	BD	120	80
	BB	180	135
Fatigue	FB	56/1800*	-
	FD	-	25/1800*
Composite Box	CD	236.5	-
	CB	550	462
	CD	282.5	199.5

*Range of torsion in kip-in.

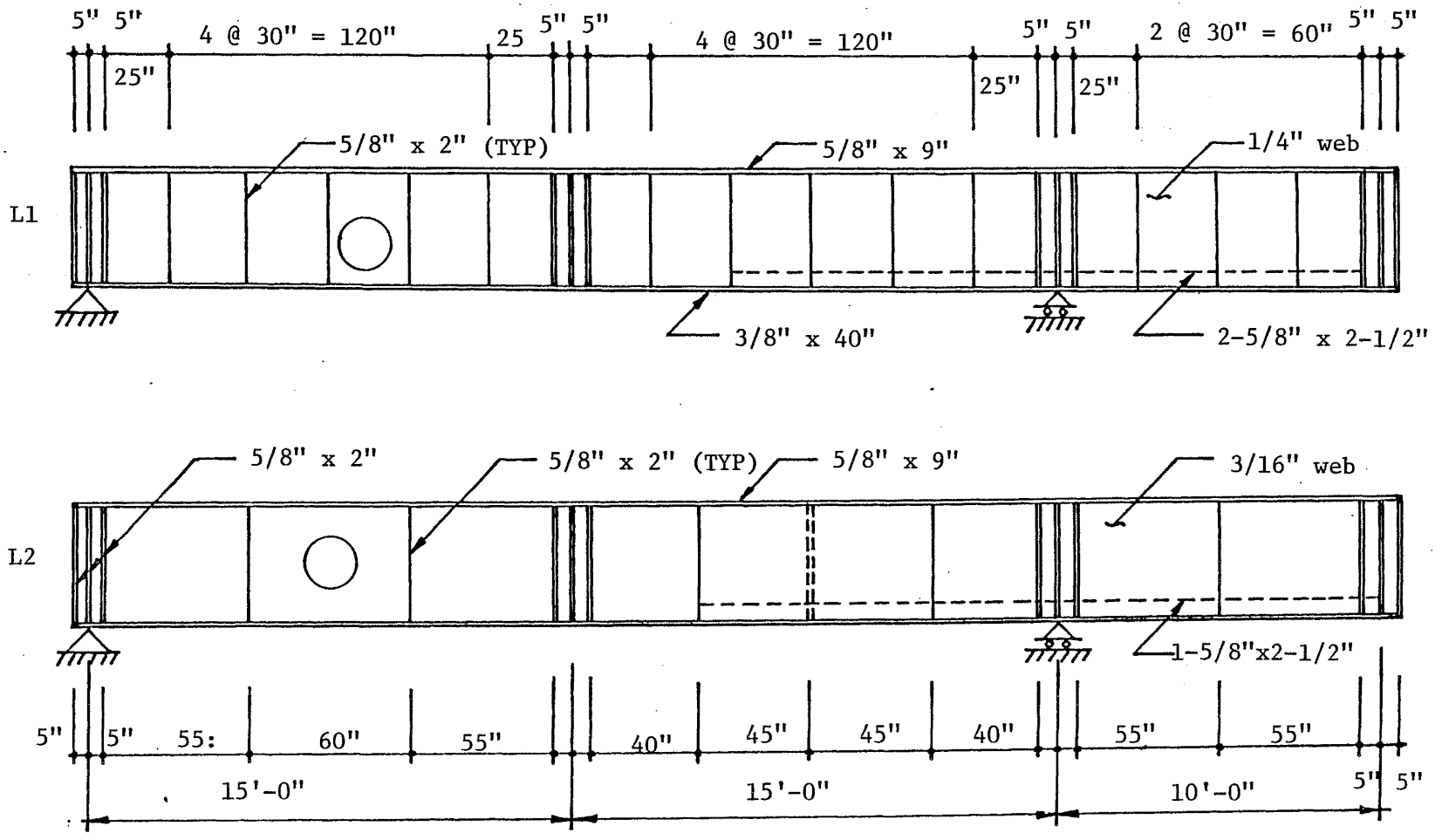

Fig. 2.1 Elevation of L1 and L2

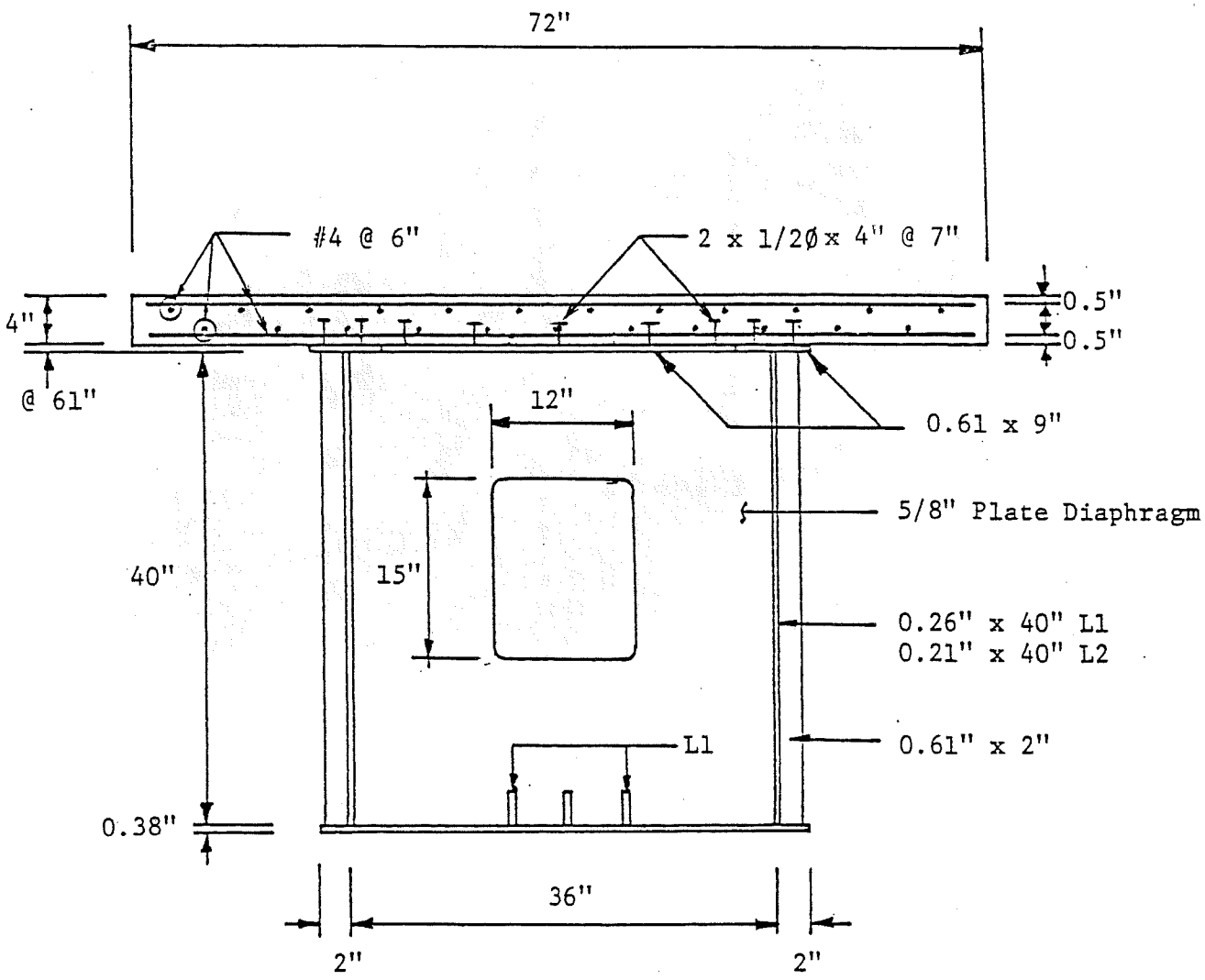

Fig. 2.2 Cross-Section of L1 and L2

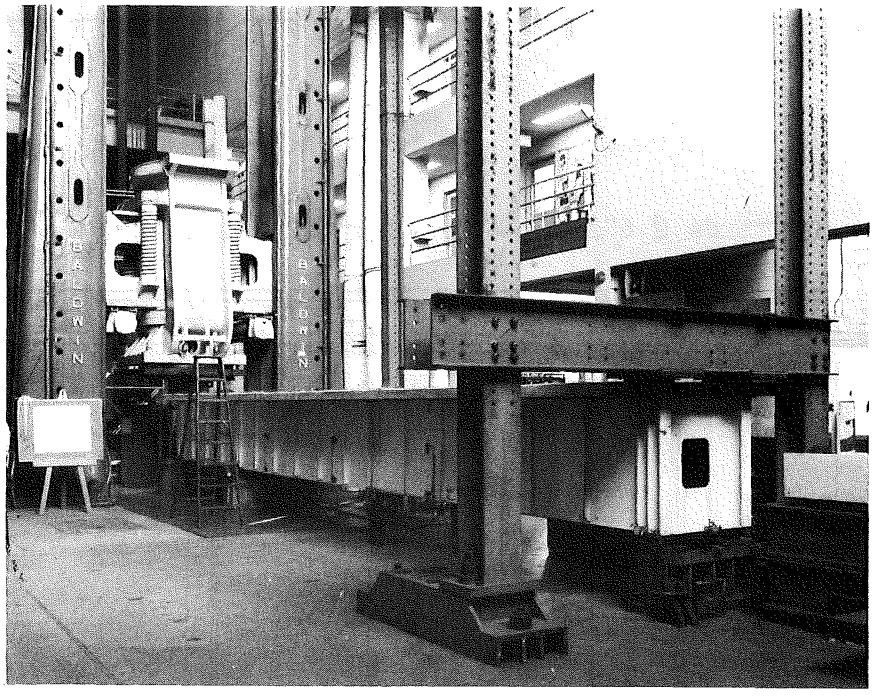

Fig. 2.3 Test Setup - Negative Bending plus Torsion

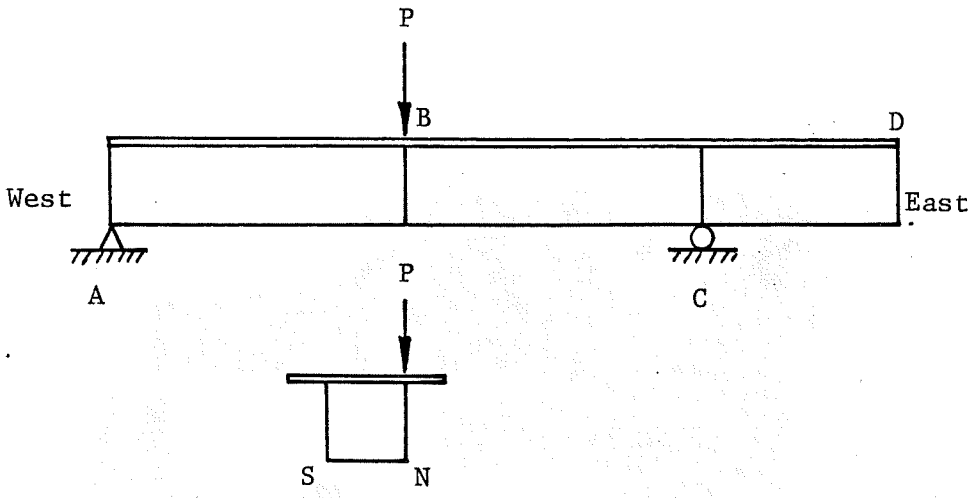

CB - Composite Box Load at B

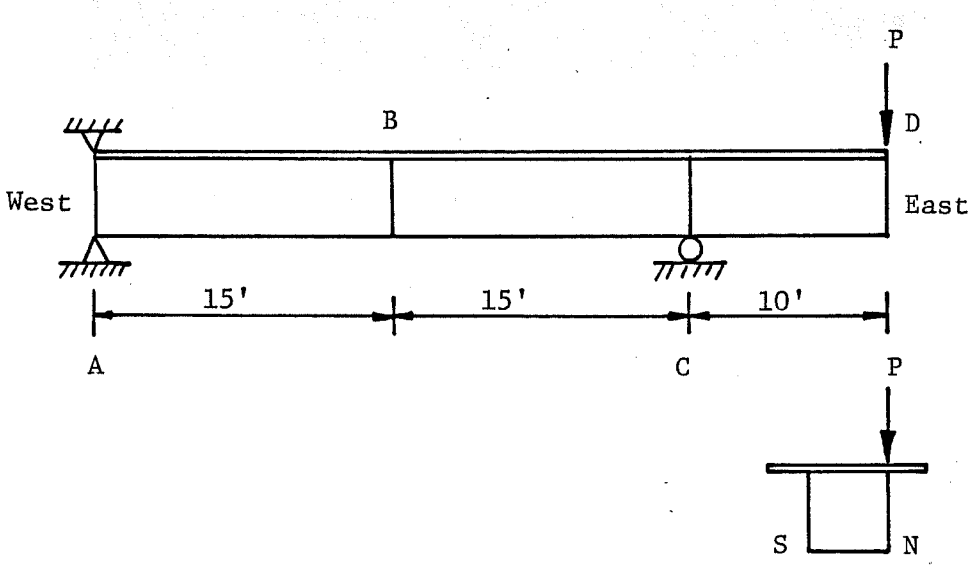

CD - Composite Box Load at D

Fig. 2.4 Schematic of Test Setup

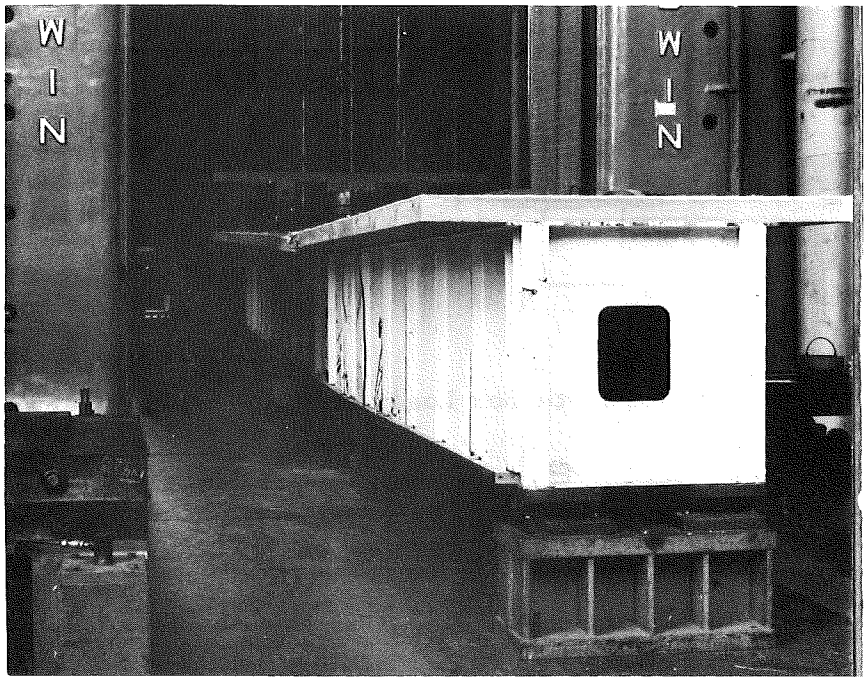

Fig. 2.5 Specimen in Position After Loading in Positive Bending and Torsion (L1 - CB)

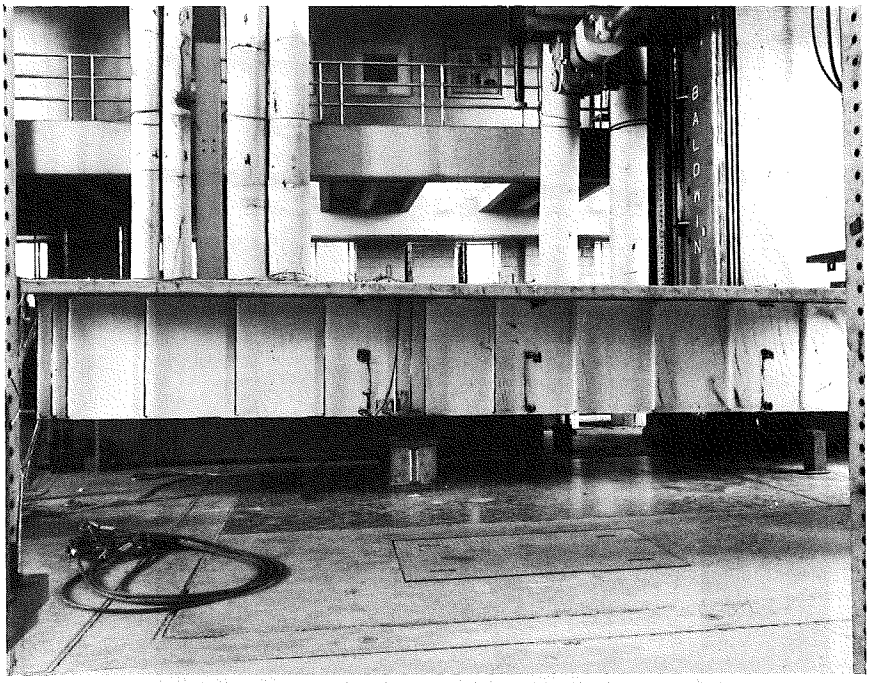

Fig. 2.6 Overhanging End of Test (L1 - CB)

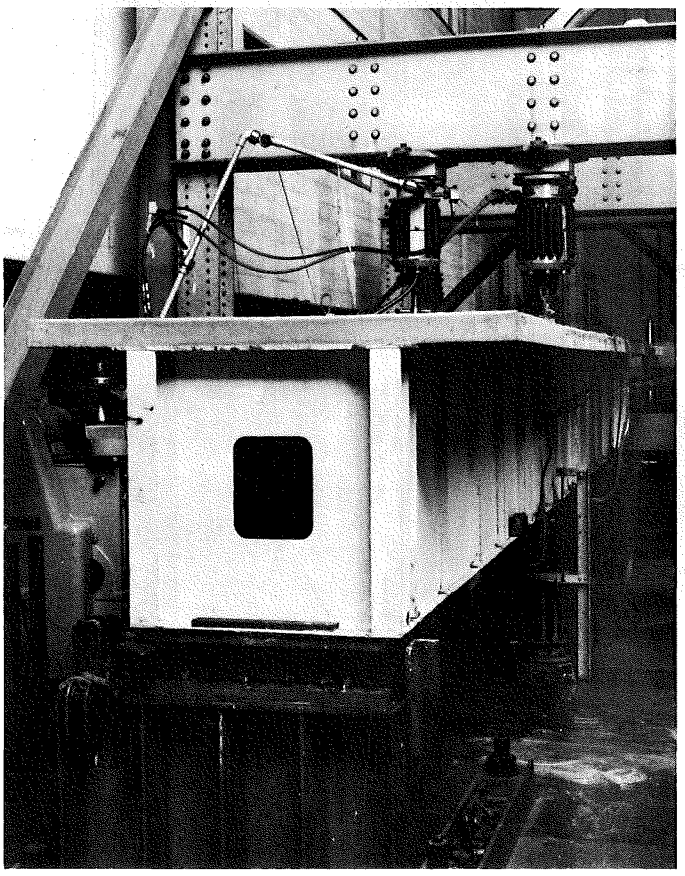

Fig. 2.7 Test Setup for Fatigue Loading
(L1 - FB)

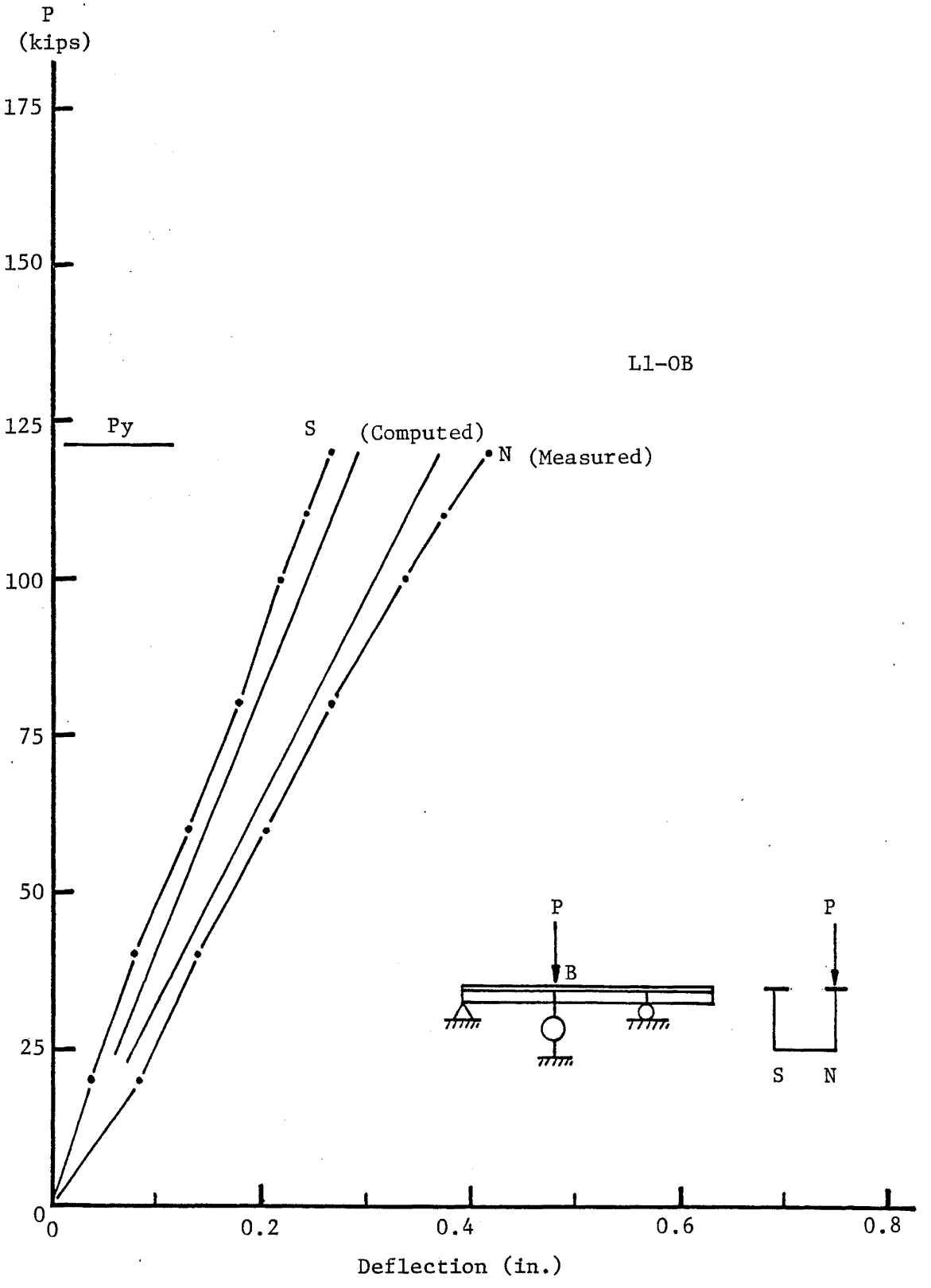

Fig. 3.1 Load versus Deflection, L1, Open U-shape Positive Bending and Torsion

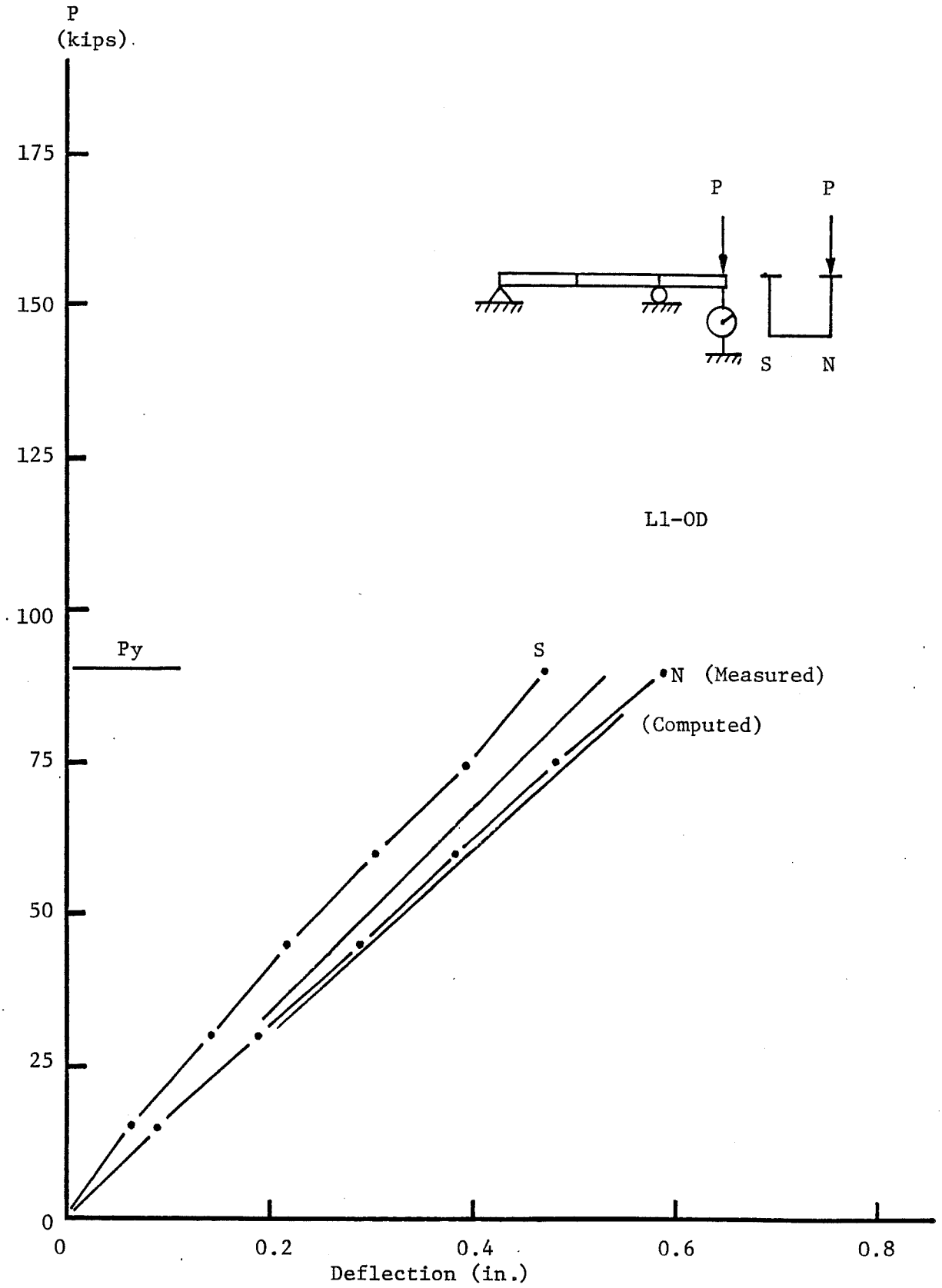

Fig. 3.2 Load versus Deflection, L1, Open U-shape, Negative Bending and Torsion

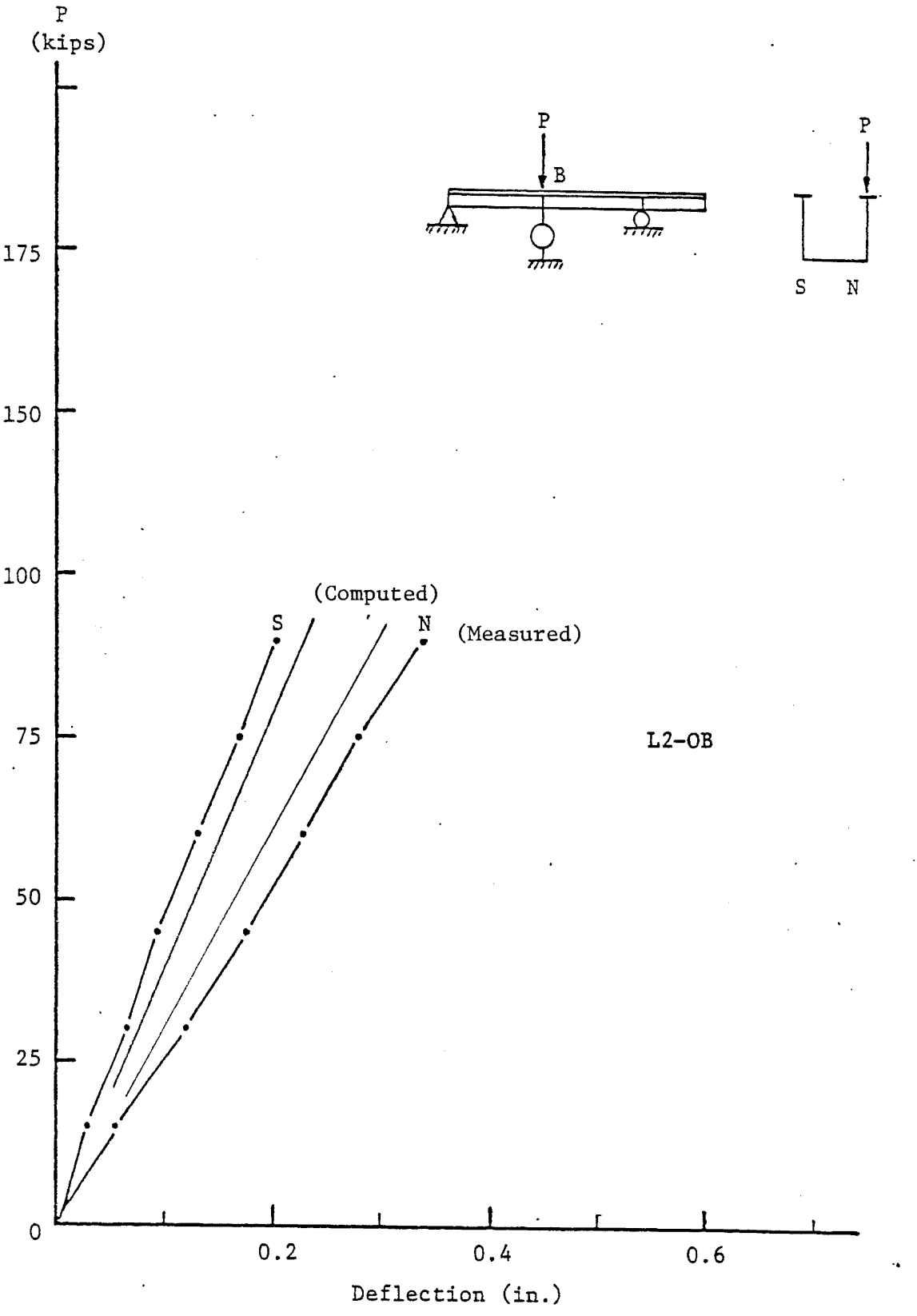

Fig. 3.3 Load versus Deflection L2-OB

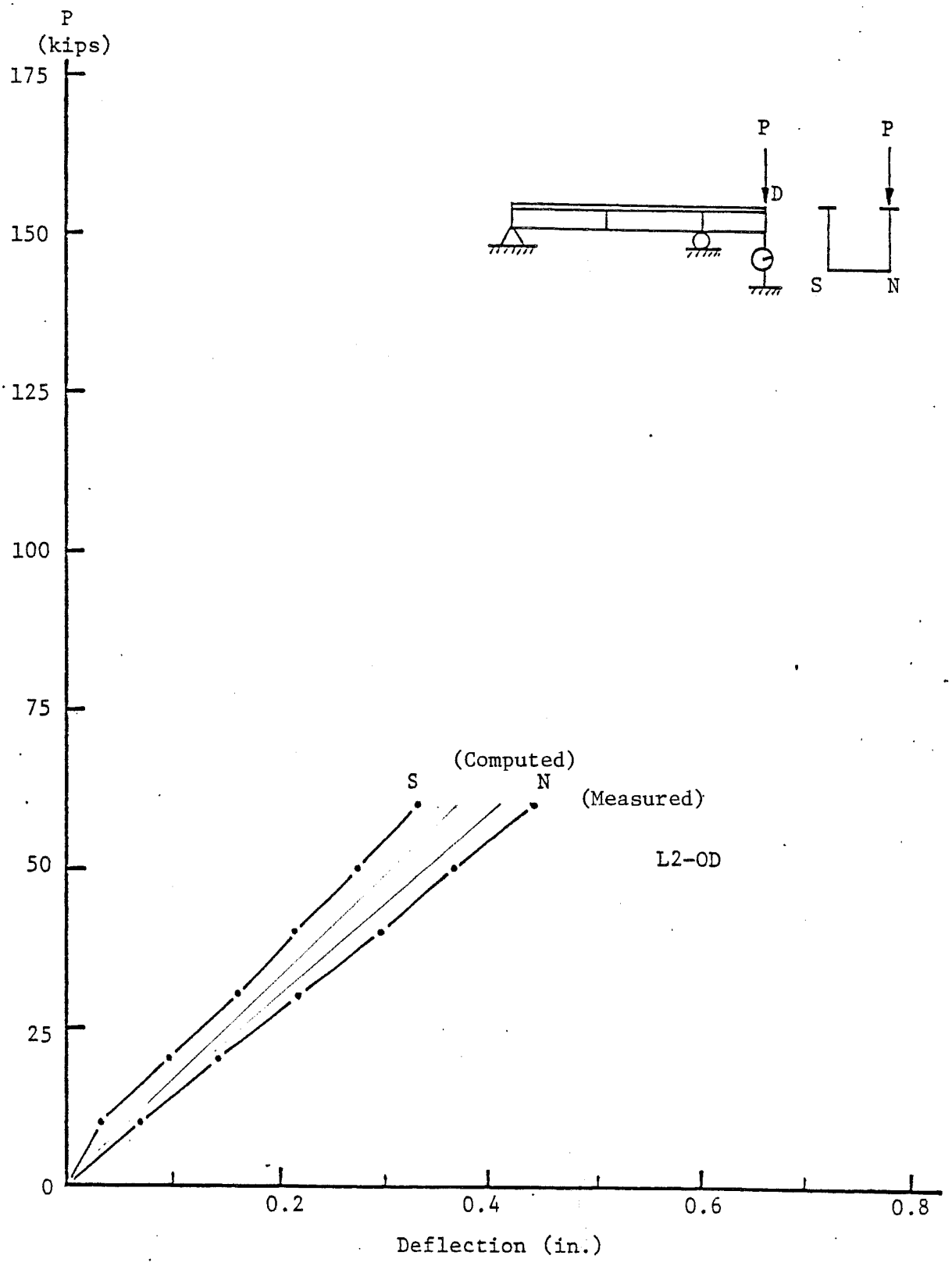

Fig. 3.4 Load versus Deflection, L2-OD

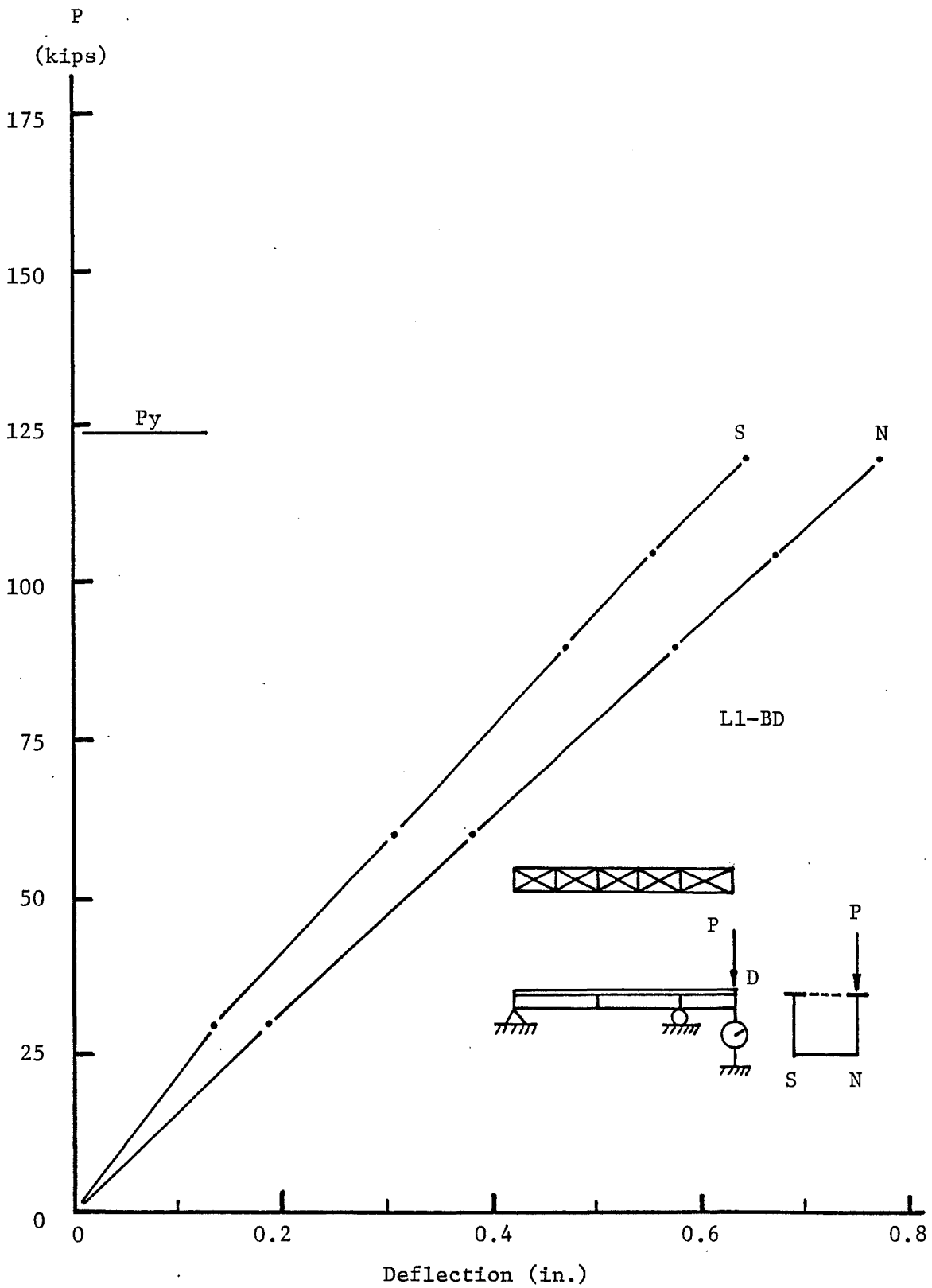

Fig. 3.5 Load versus Deflection, L1, Braced U-shape Negative Bending and Torsion

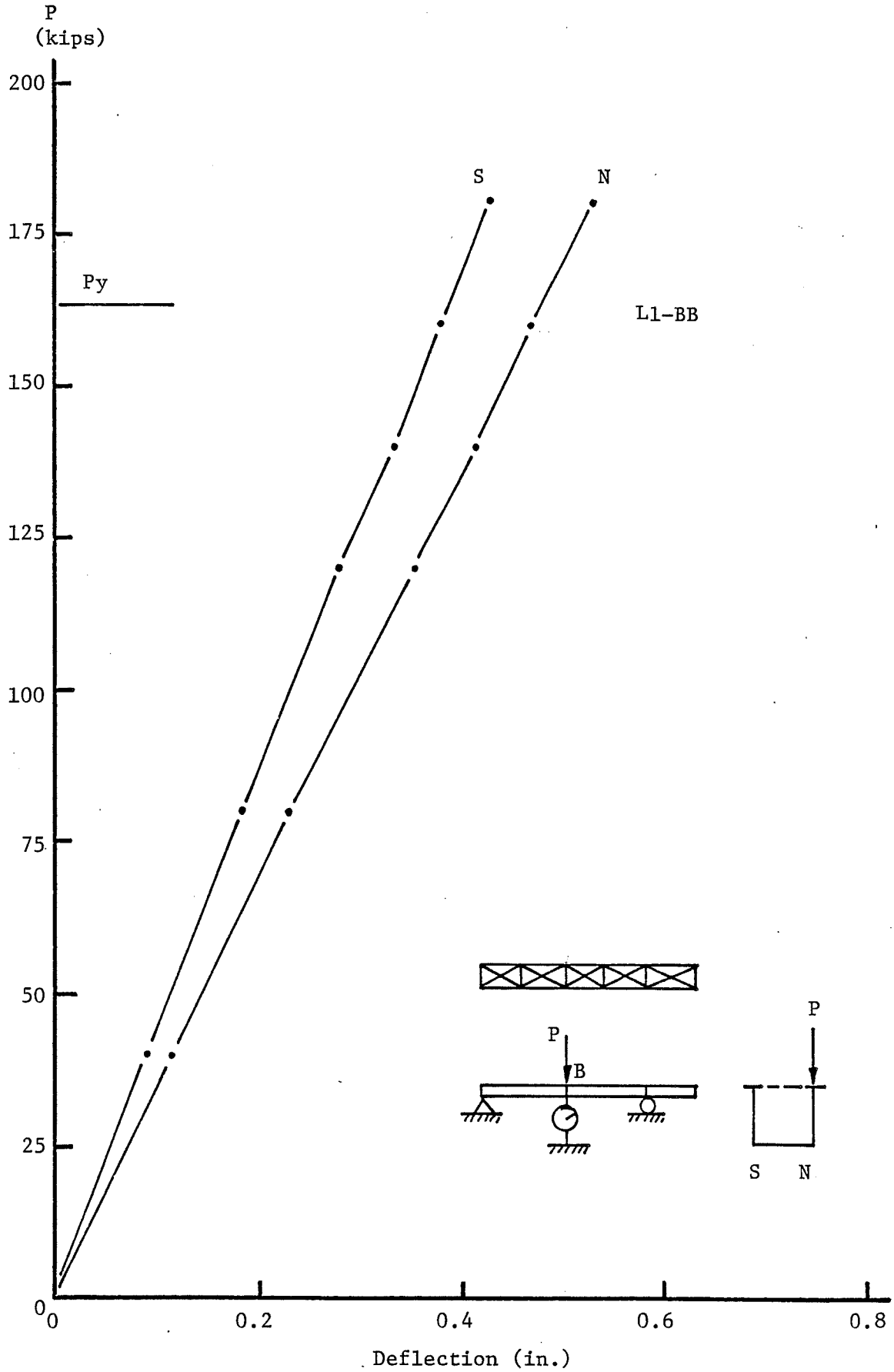

Fig. 3.6 Load versus Deflection, L1, Braced U-shape, Positive Bending and Torsion

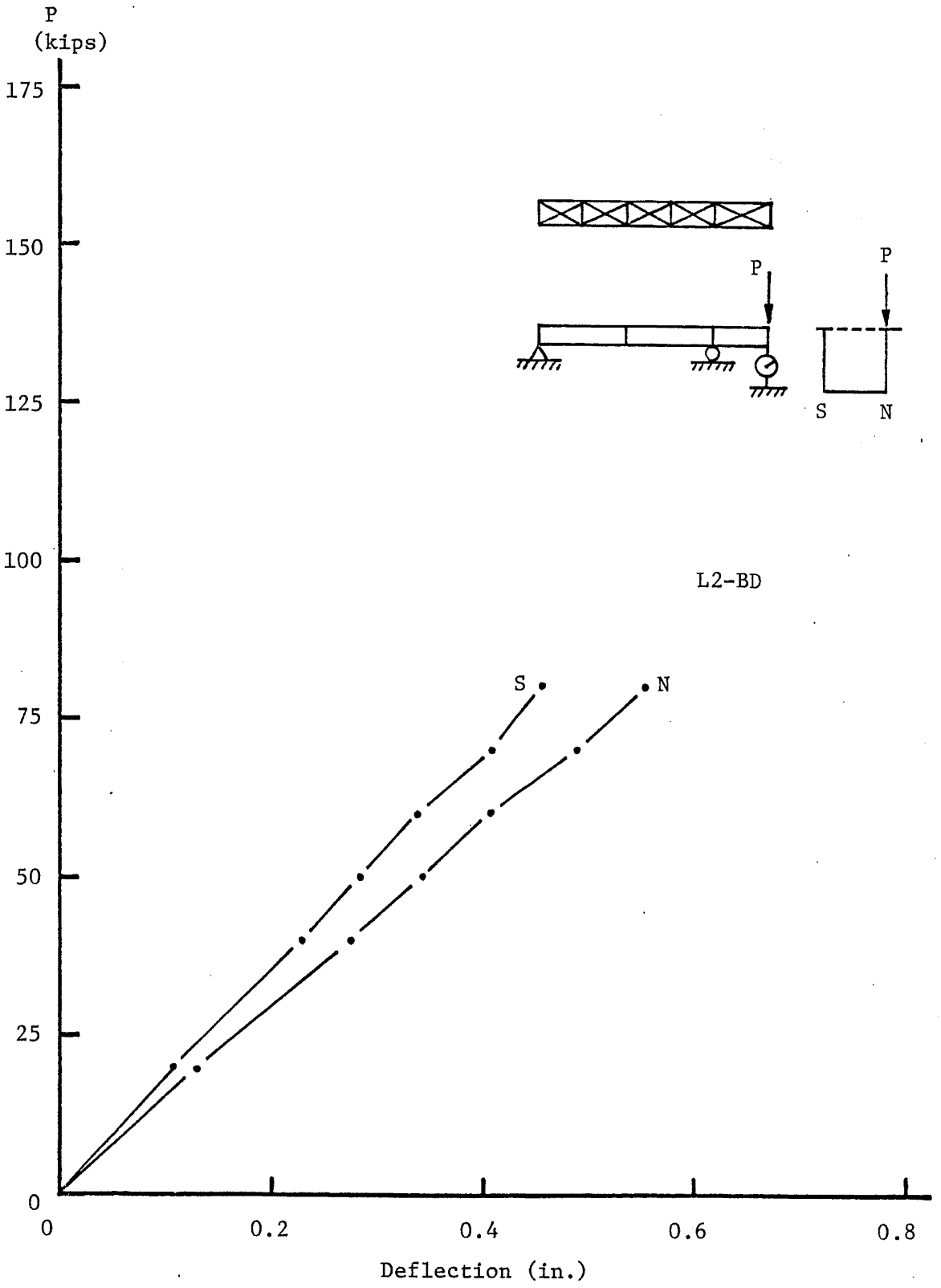

Fig. 3.7 Load versus Deflection, L2-BD

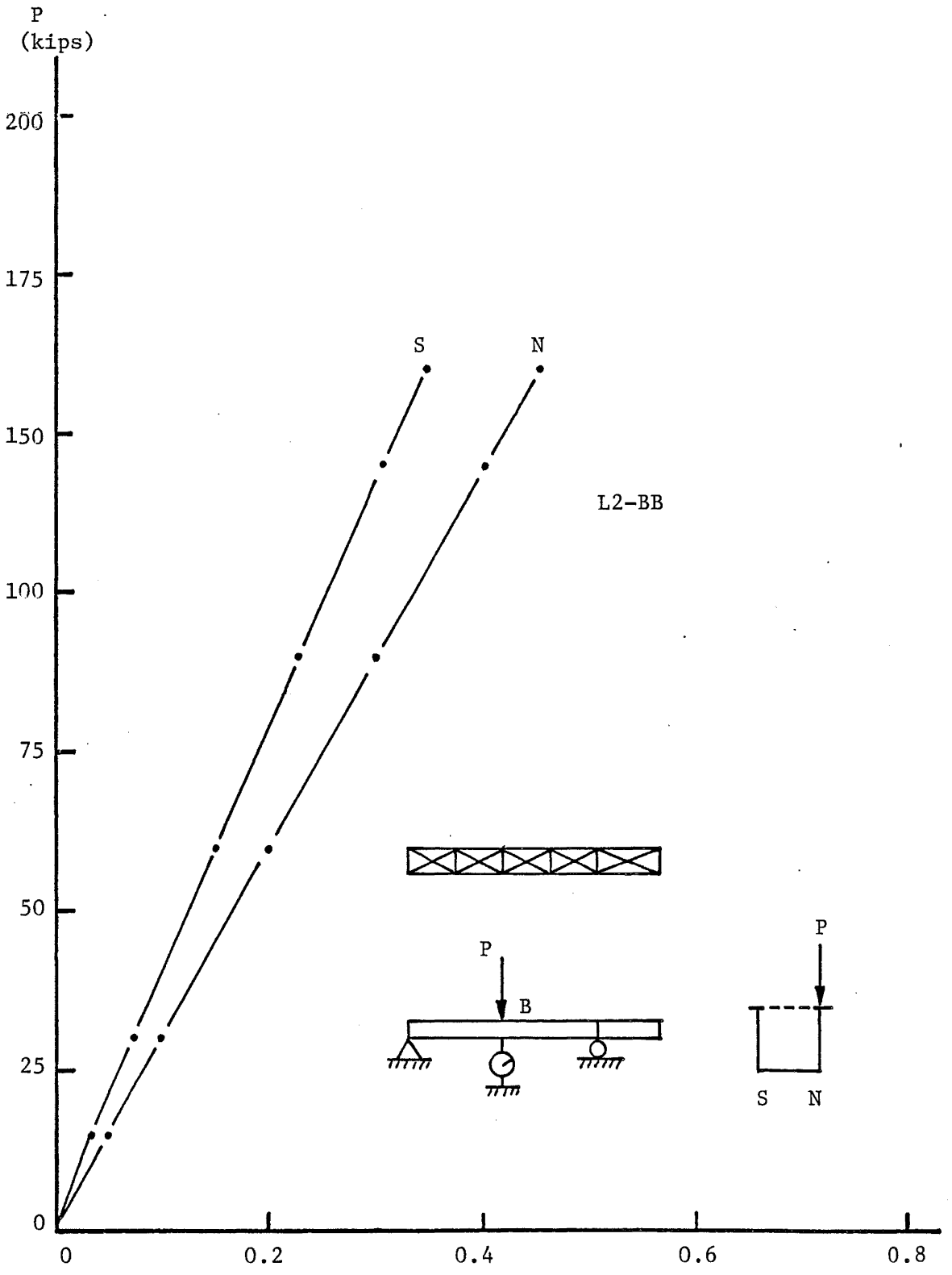

Fig. 3.8 Load versus Deflection, L2-BB

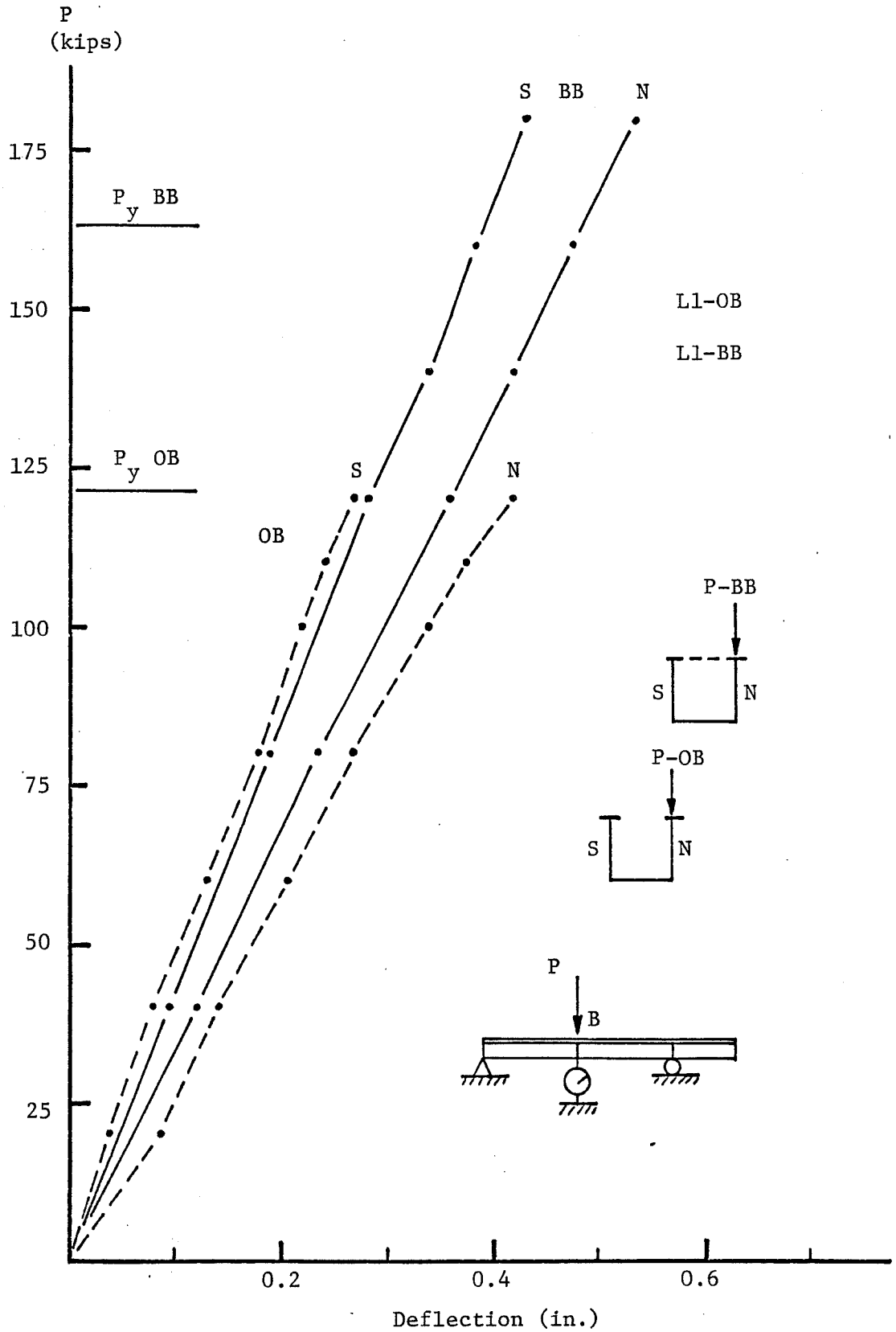

Fig. 3.9 Comparison of Deflection, Open and Braced U-shape, L1

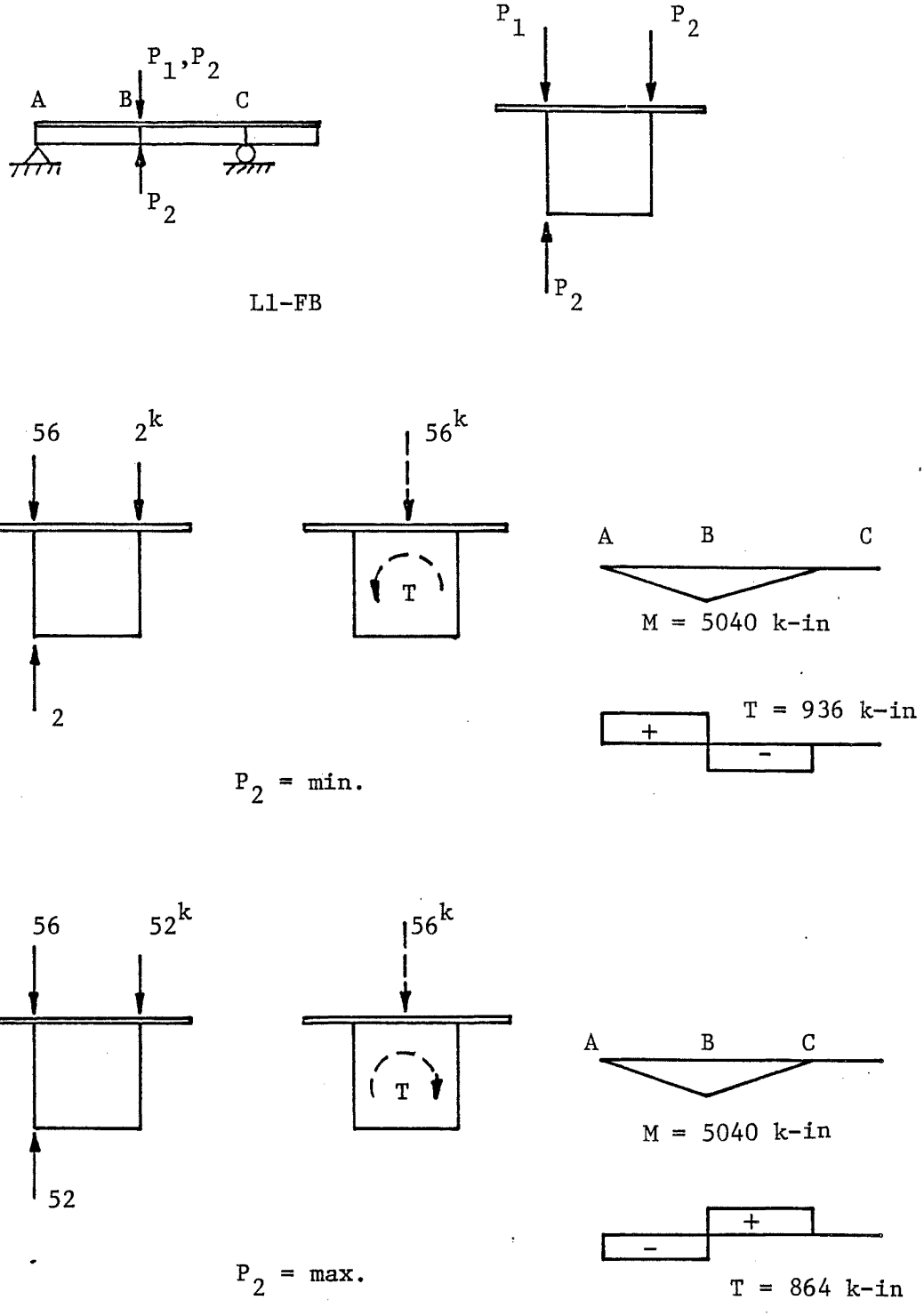

Fig. 3.10 Bending Moment and Torsional Loads, Fatigue Loading, L1-FB

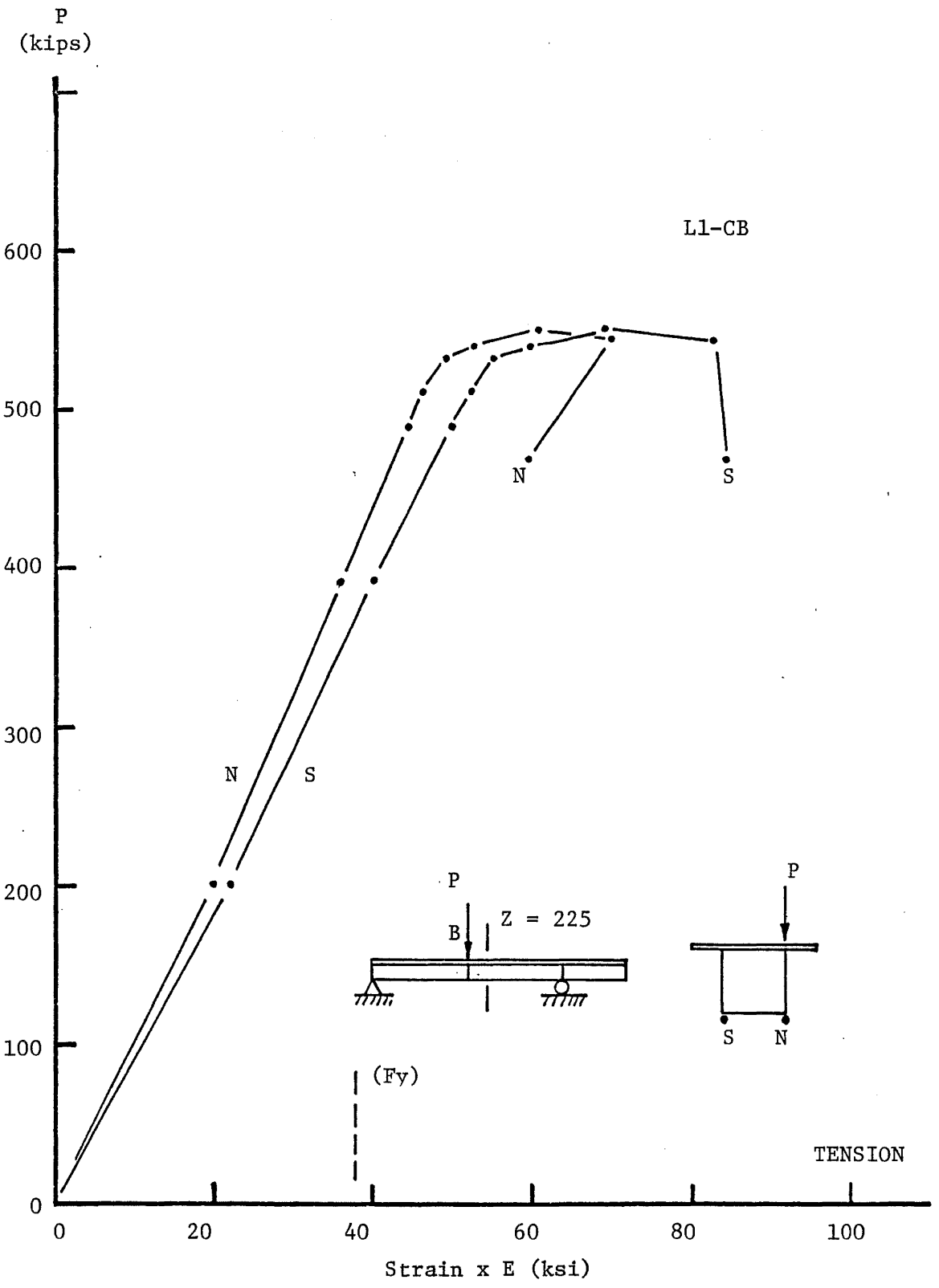

Fig. 4.1 Strains in Bottom Flange under Web, Composite Box Girder Test L1-CB

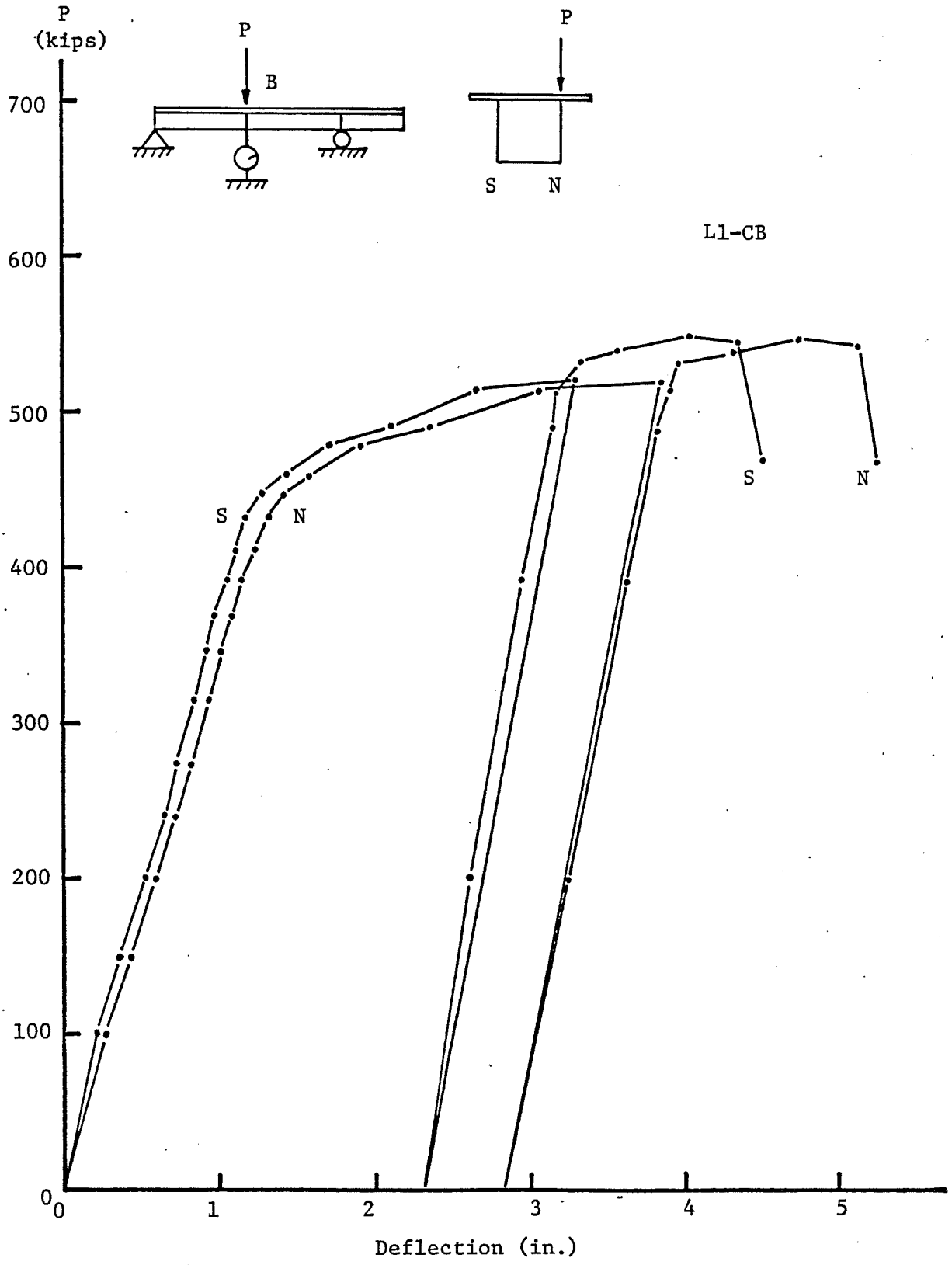

Fig. 4.2 Load-Deflection Curves, Composite Box Girder Test L1-CB

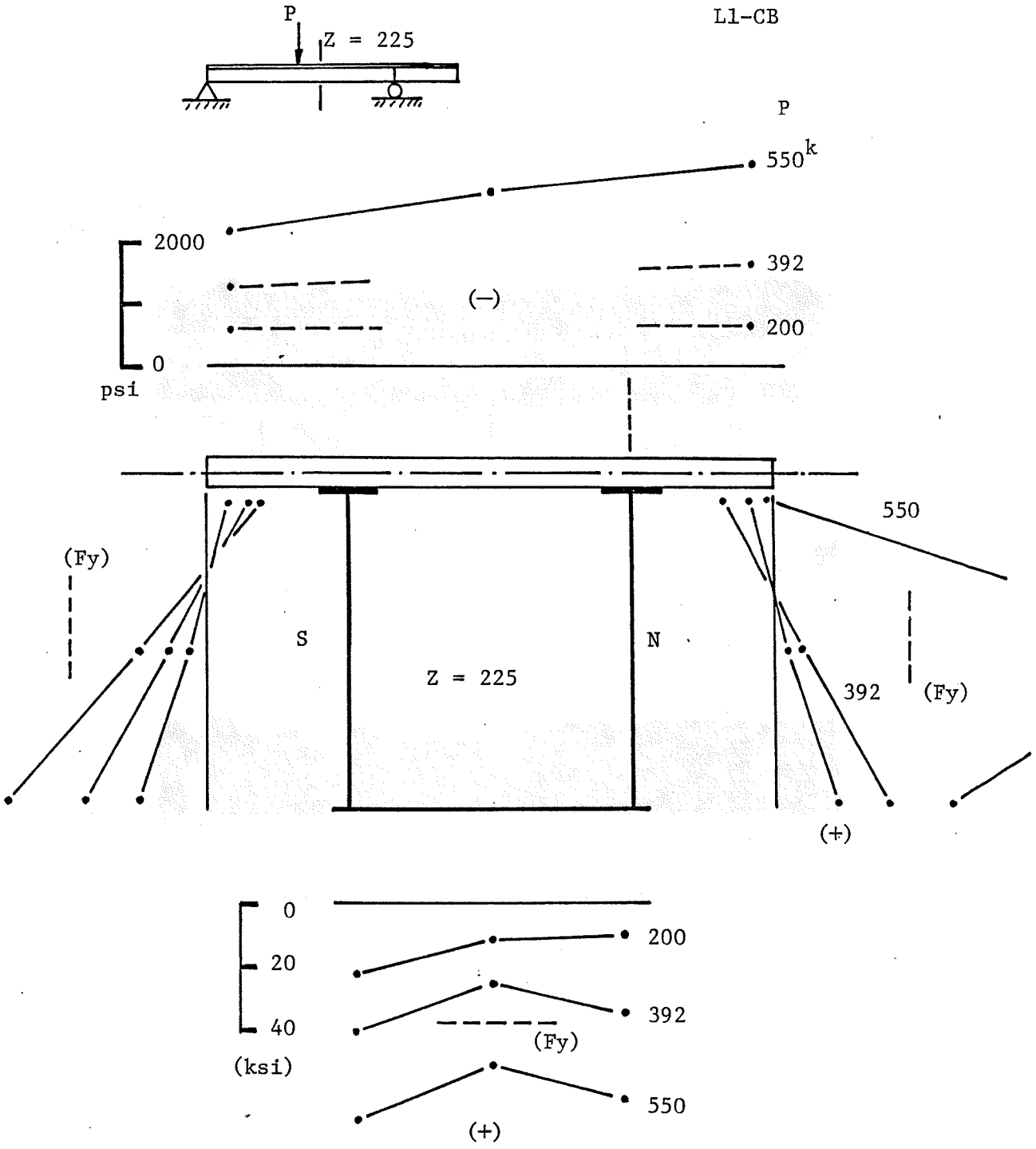

Fig. 4.3 Stress Distribution, Cross Section Z = 225 in., Test L1-CB

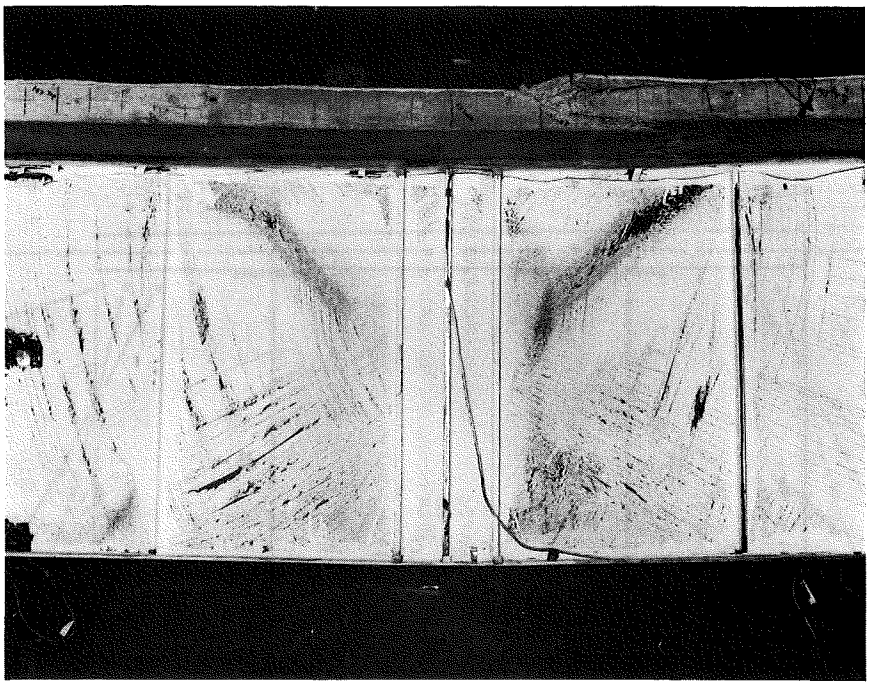

Fig. 4.4 Failure of Composite Box Grider

Test L1 - CB

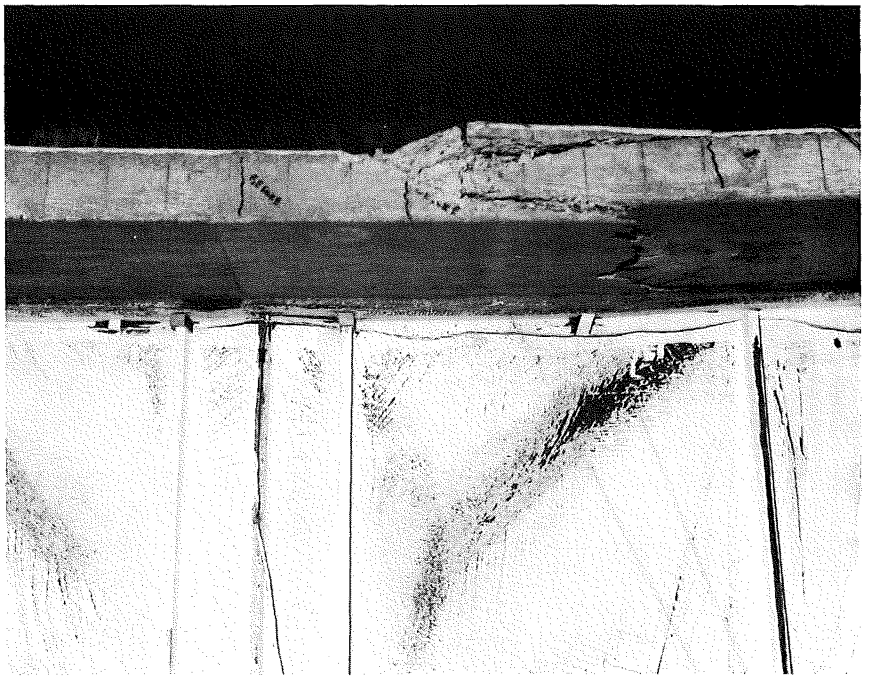

Fig. 4.5 Crushed Concrete Deck, Test L1 - CB

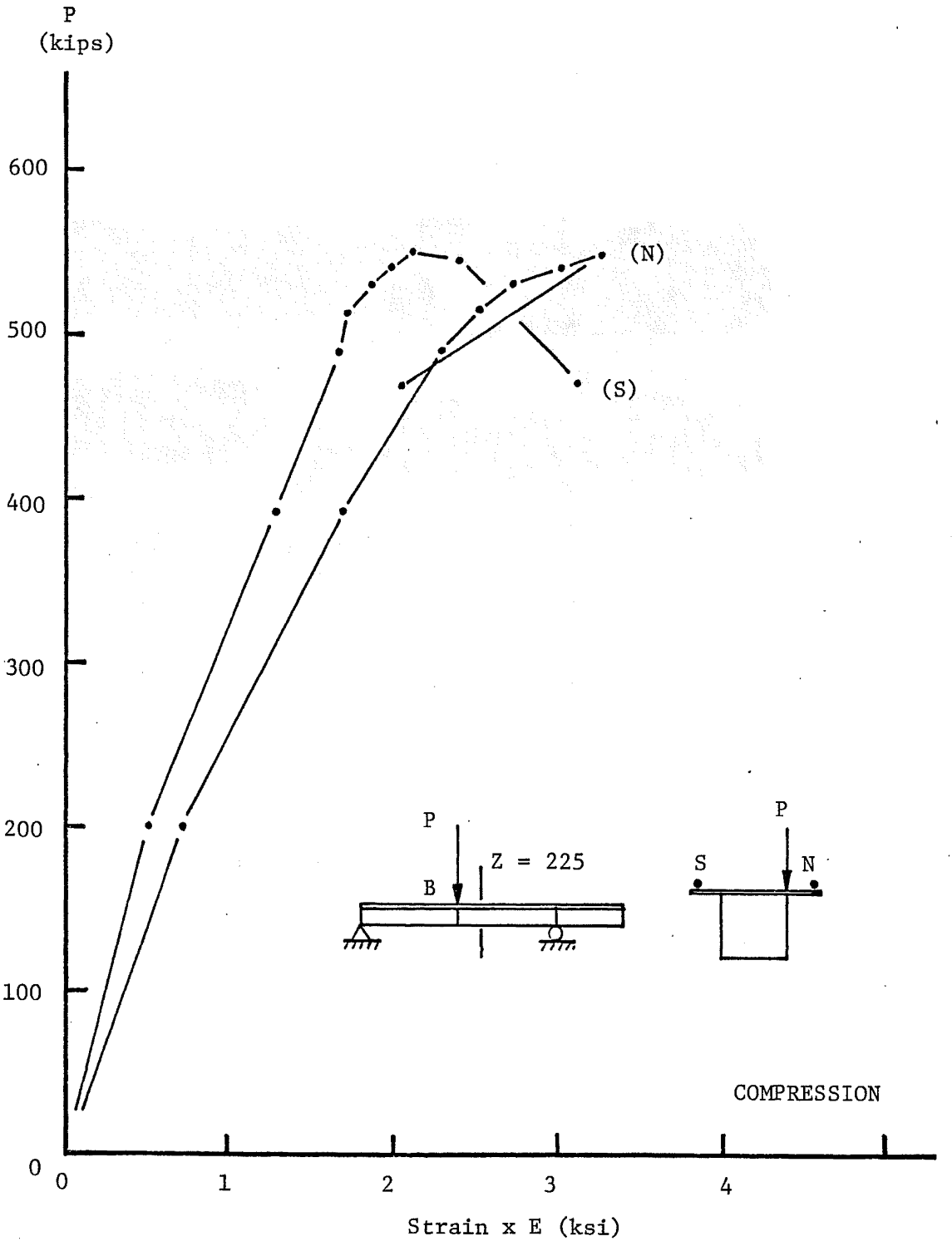

Fig. 4.6 Average Strains in Concrete Deck, Z = 225 in., Test L1-CB

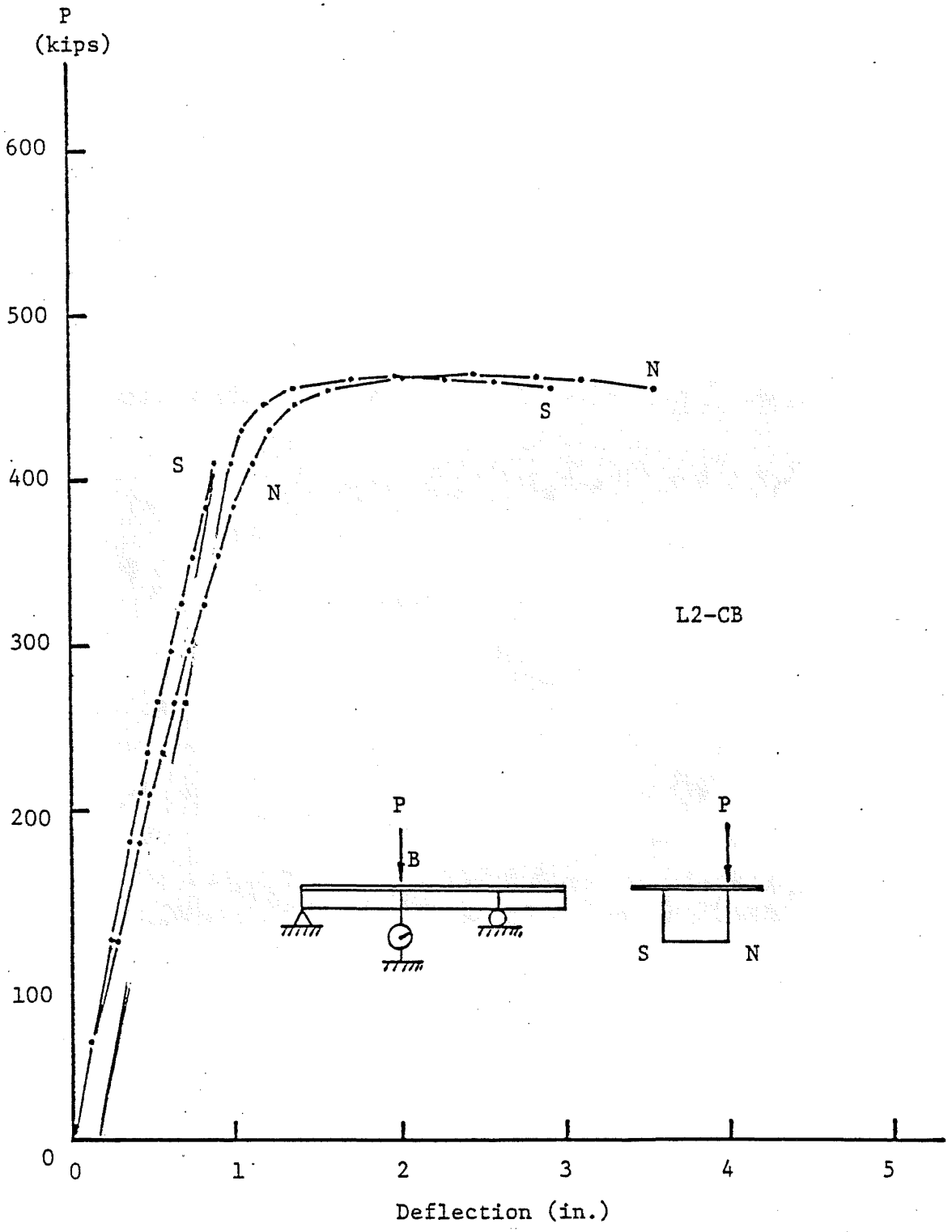

Fig. 4.7 Load-Deflection Curves, Composite Box Girder Test L2-CB

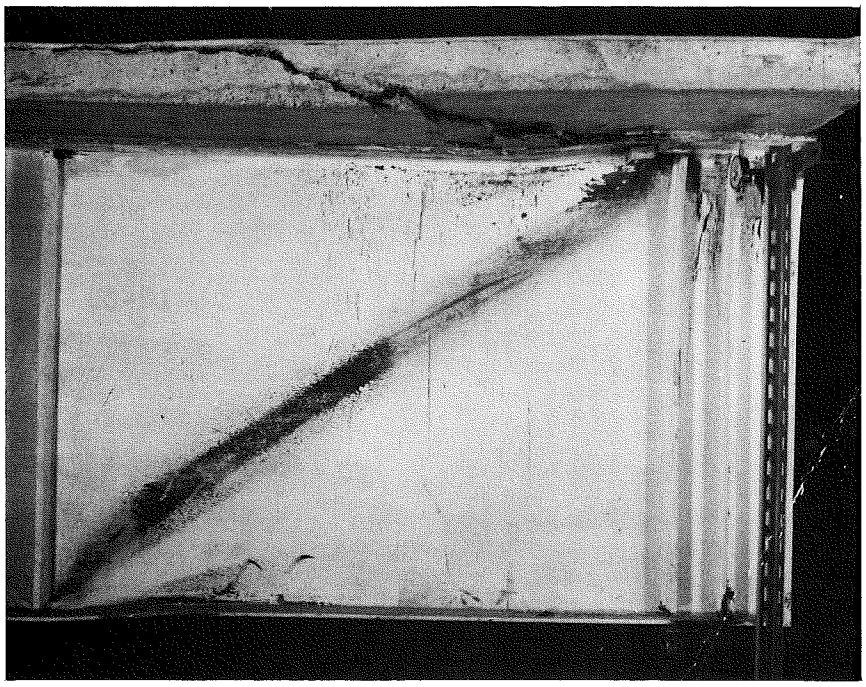

Fig. 4.8 Failed North Web and Flanges of West End Panel (L2 - CB)

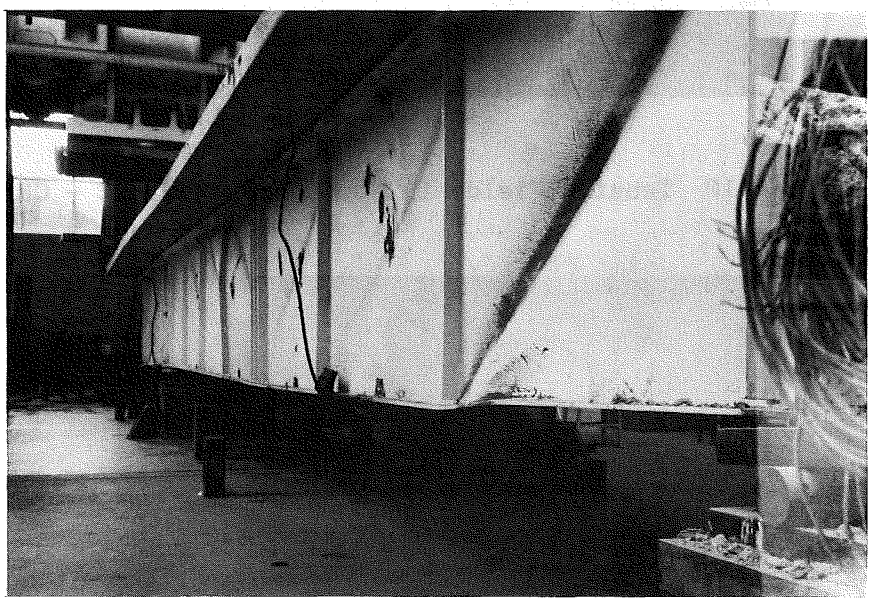

Fig. 4.9 Deflected Steel Bottom Flange
Test 12 - CB

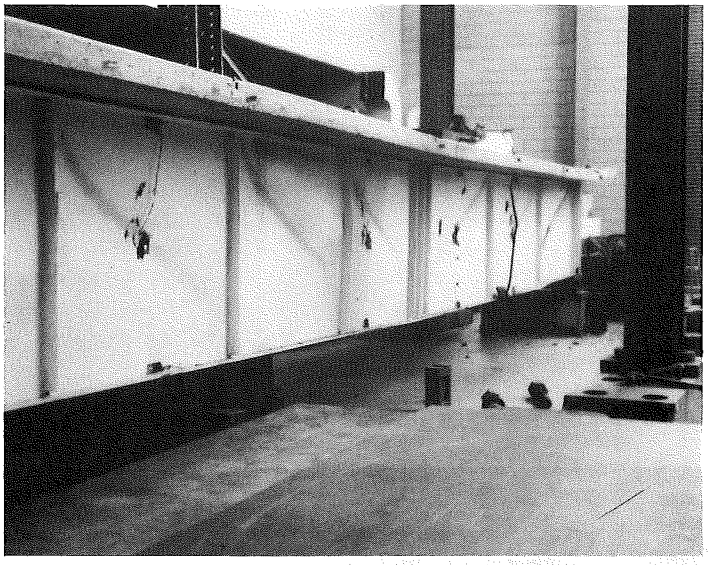

Fig. 4.10 Tension Fields in North Web, Test L2 - CB

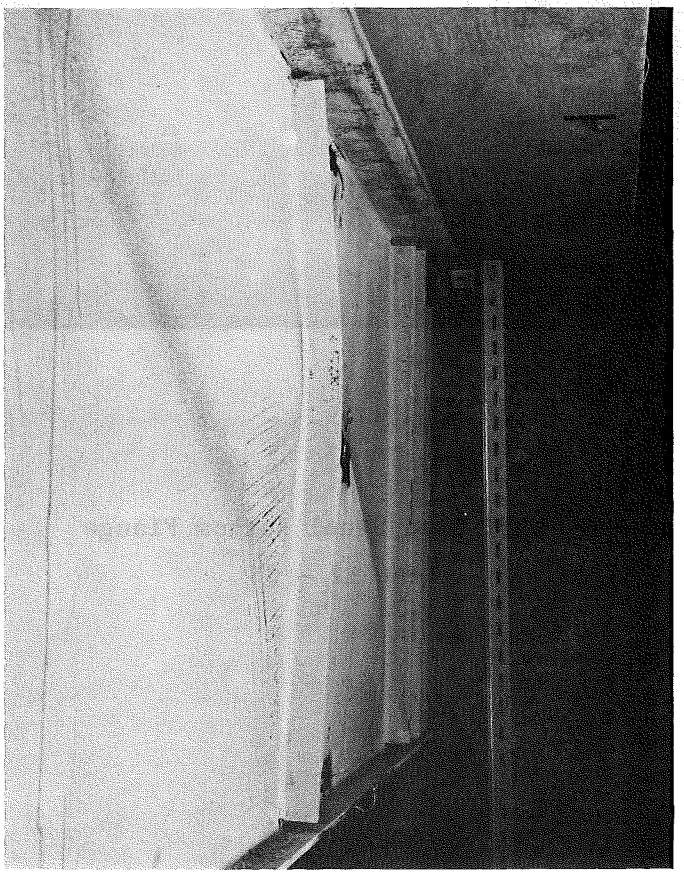

Fig. 4.11 Tension Field and Bent Stiffener, South Web, Test L2 - CB

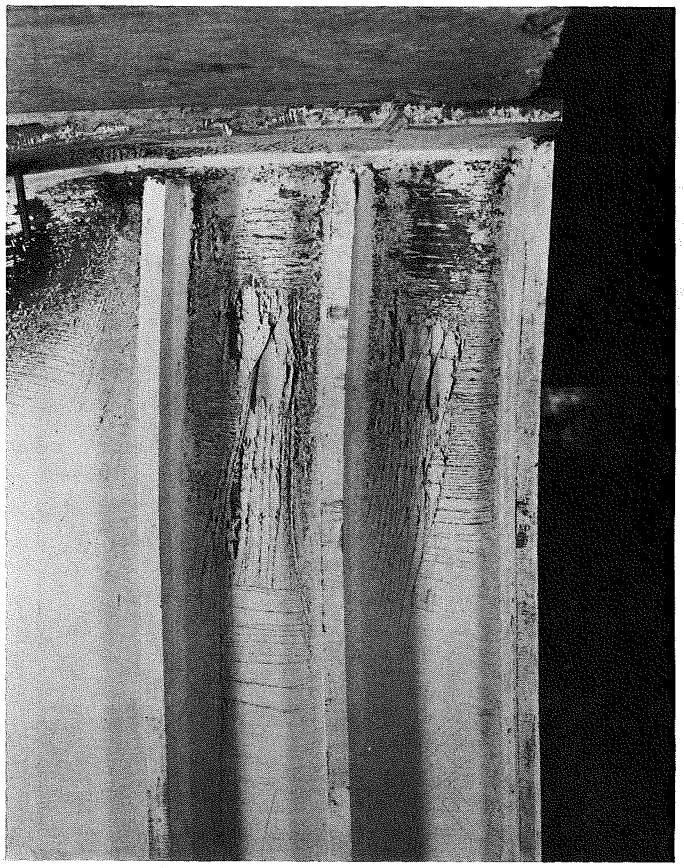

Fig. 4.12 Deformed End Bearing Stiffeners
Test L2 - CB

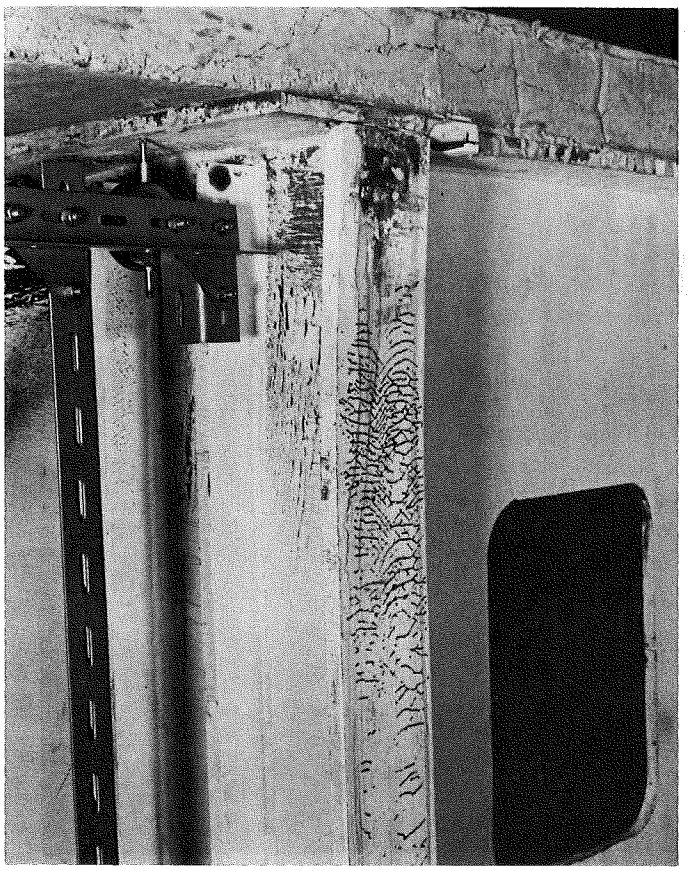

Fig. 4.13 Yield Lines on End Bearing Stiffener
Test L2 - CB

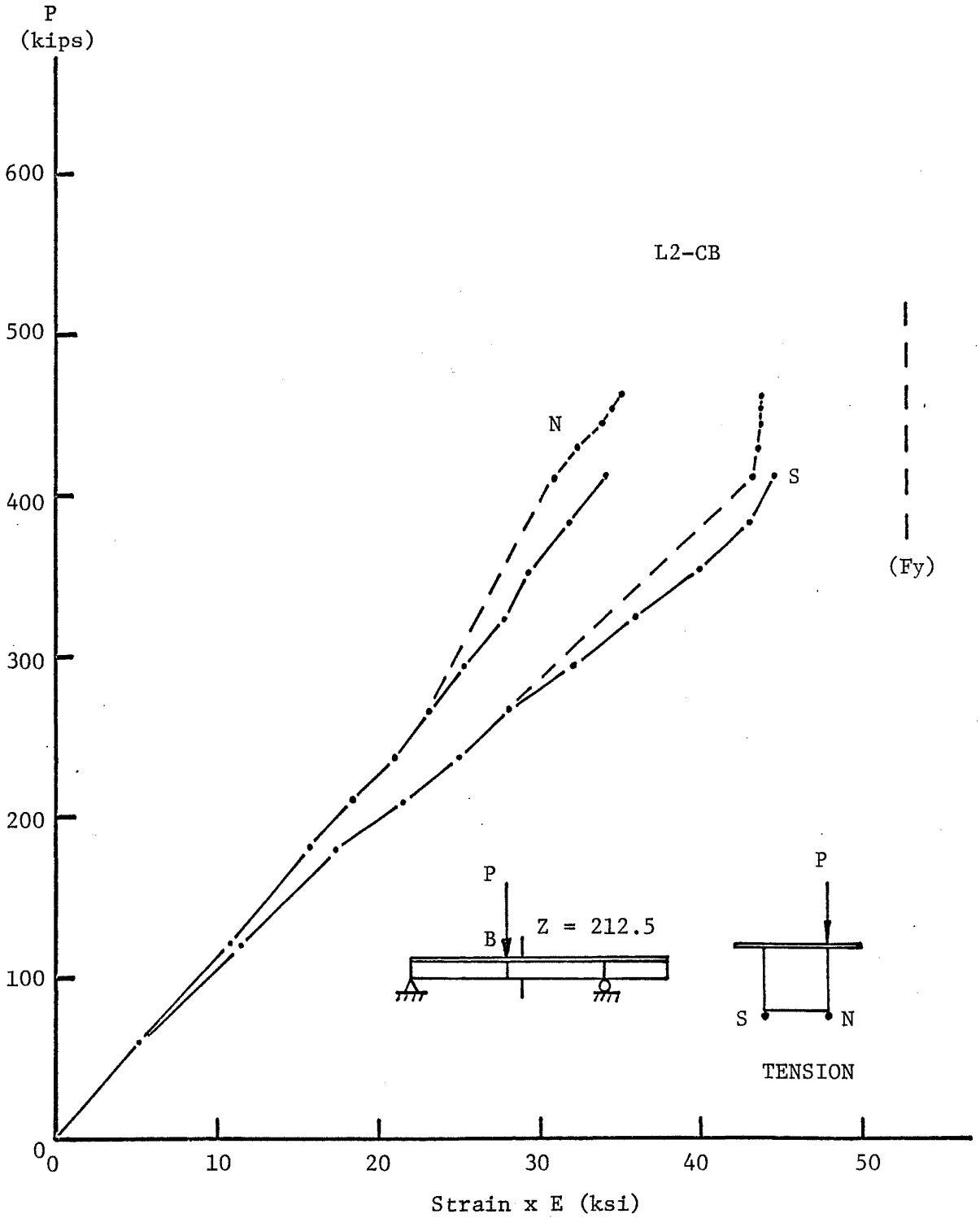

Fig. 4.14 Strain in Bottom Flange, Z = 212.5 in., Test L2-CB

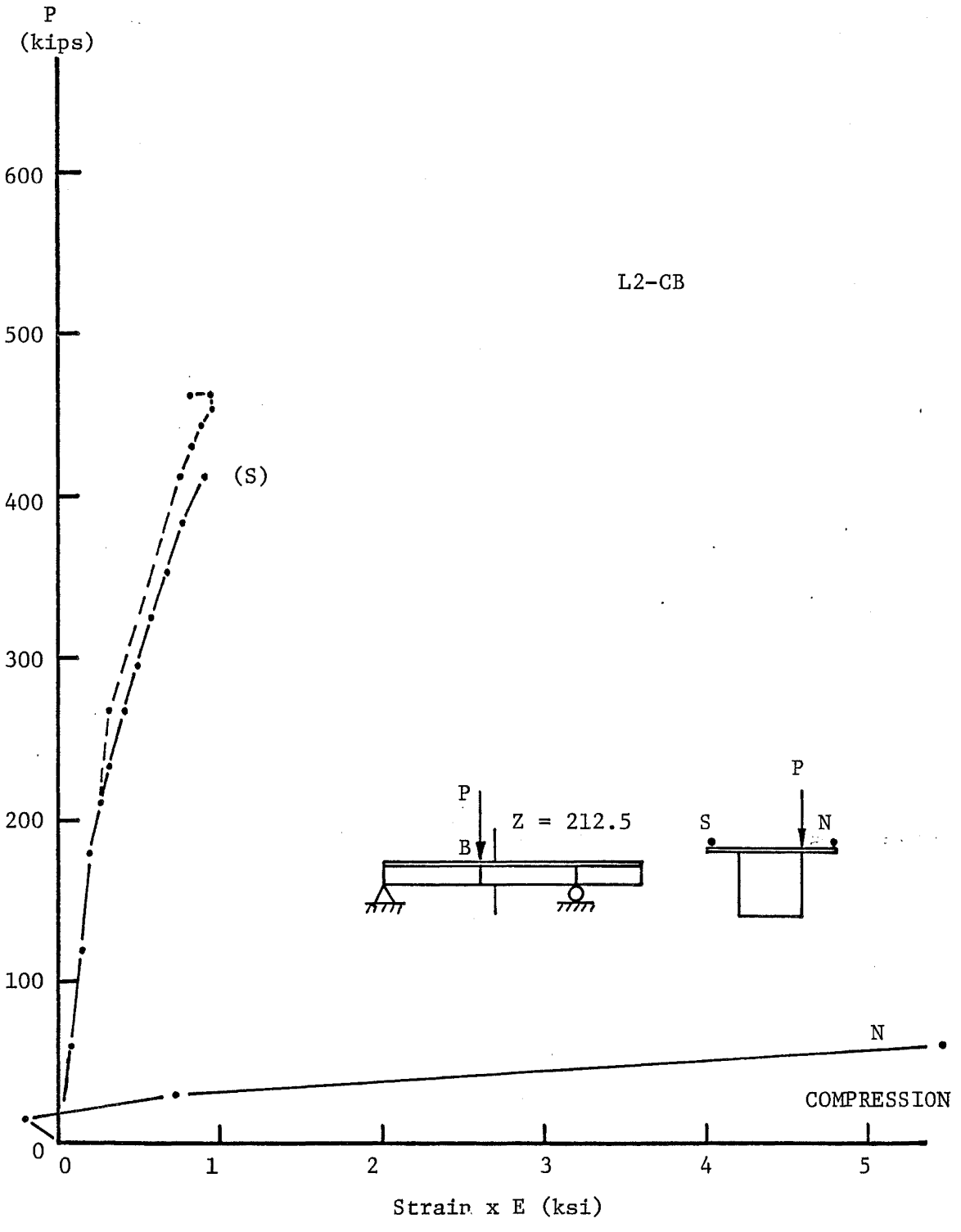

Fig. 4.15 Average Strain in Concrete Deck, Z = 212.5 in., Test L2-CB

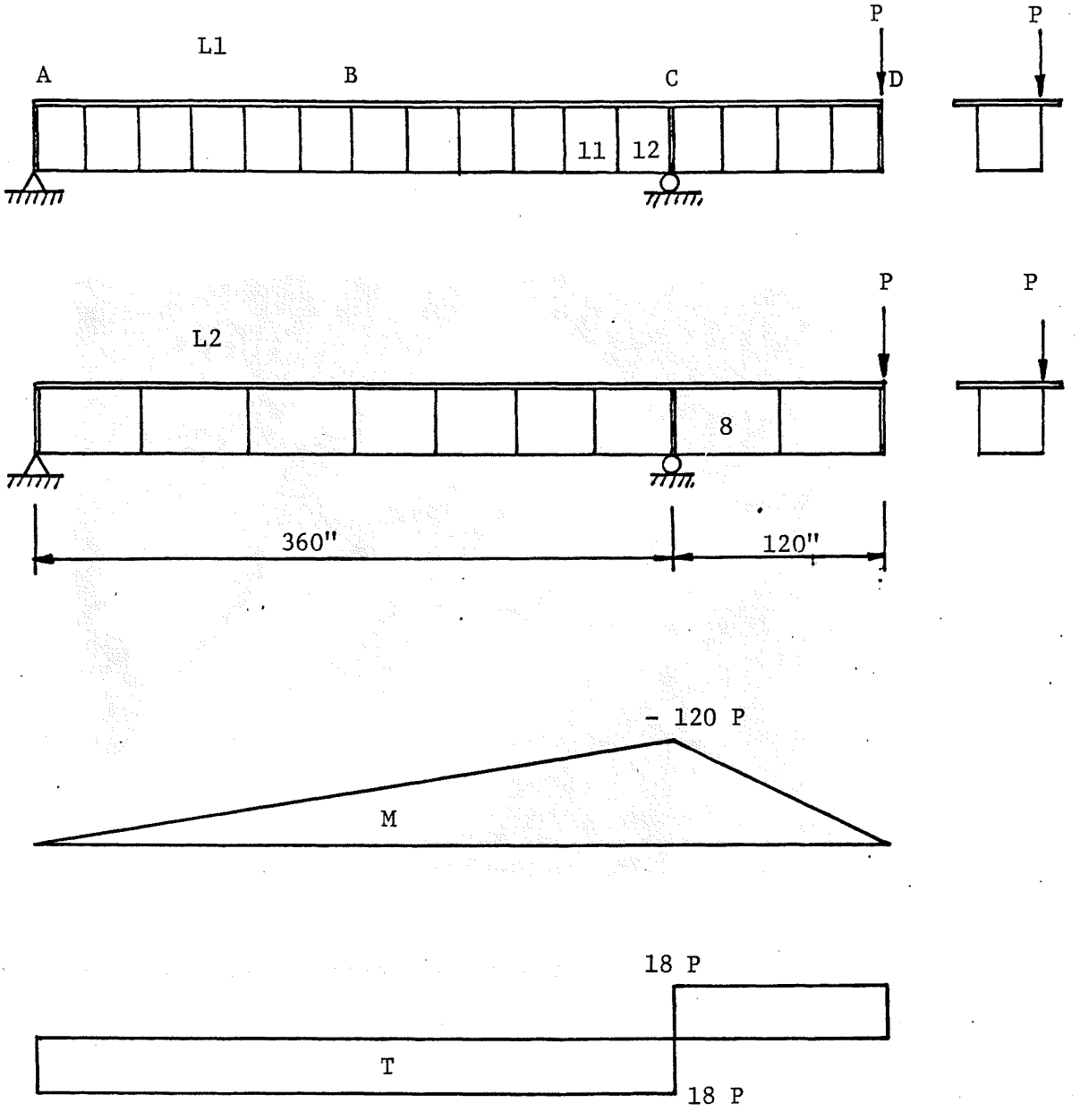

Fig. 5.1 Bending Moment and Torsion, Tests L1-CD and L2-CD

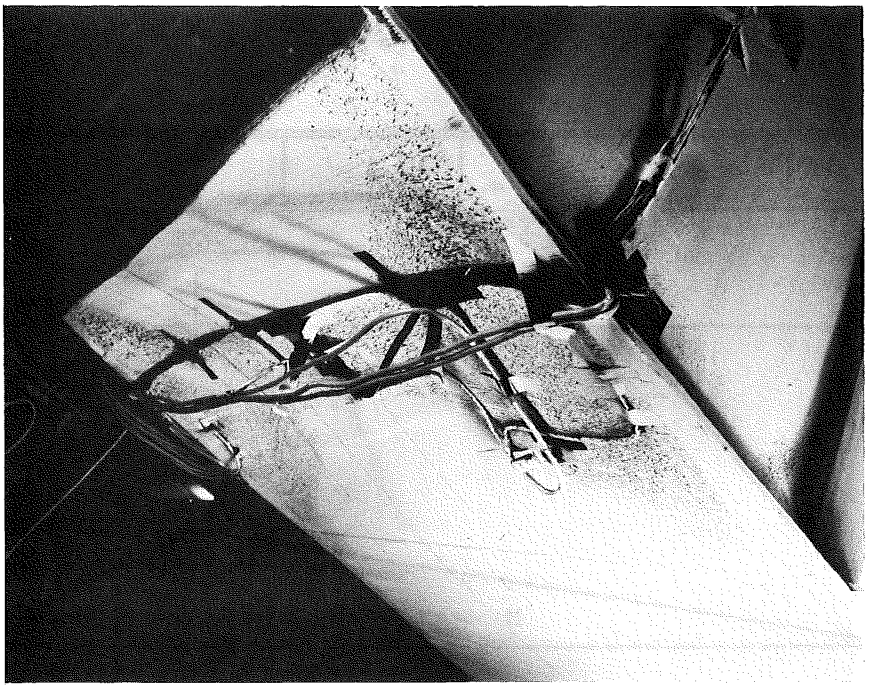

Fig. 5.2 Failed Compression Flange, Panel 11, L1-CD

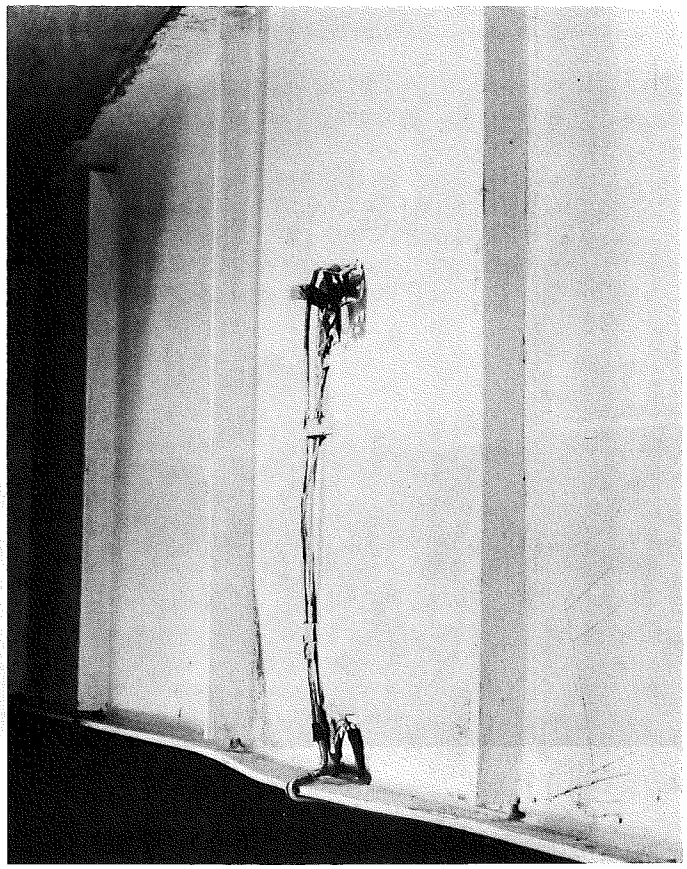

Fig. 5.3 Deflected Bottom Flange and South Web of Panel 11, L1-CD

Fig. 5.4 Yielding of Web at Bottom Flange, Panel 11, L1-CD

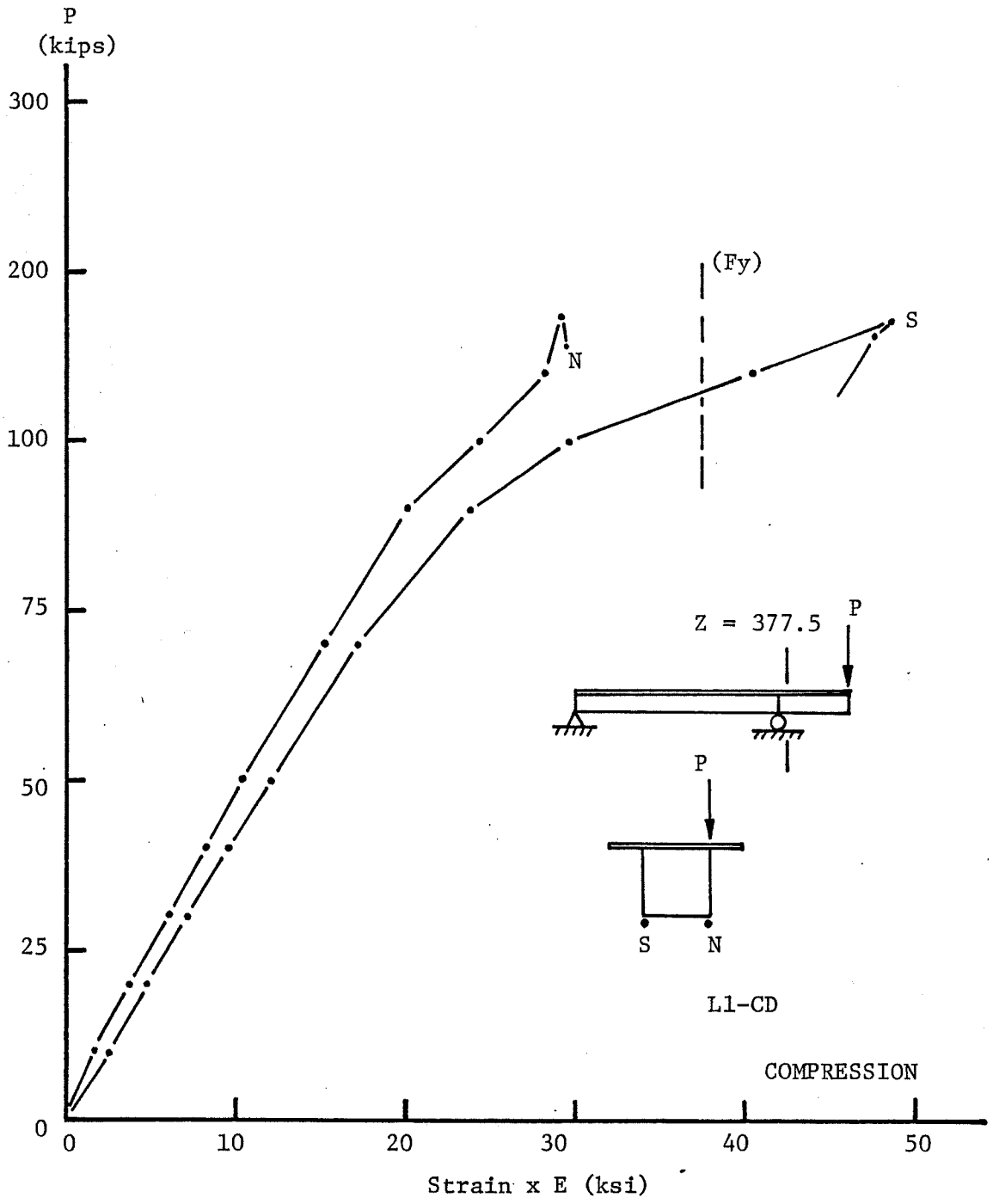

Fig. 5.5 Strain in Bottom Flange, Z = 377.5 in., L1-CD

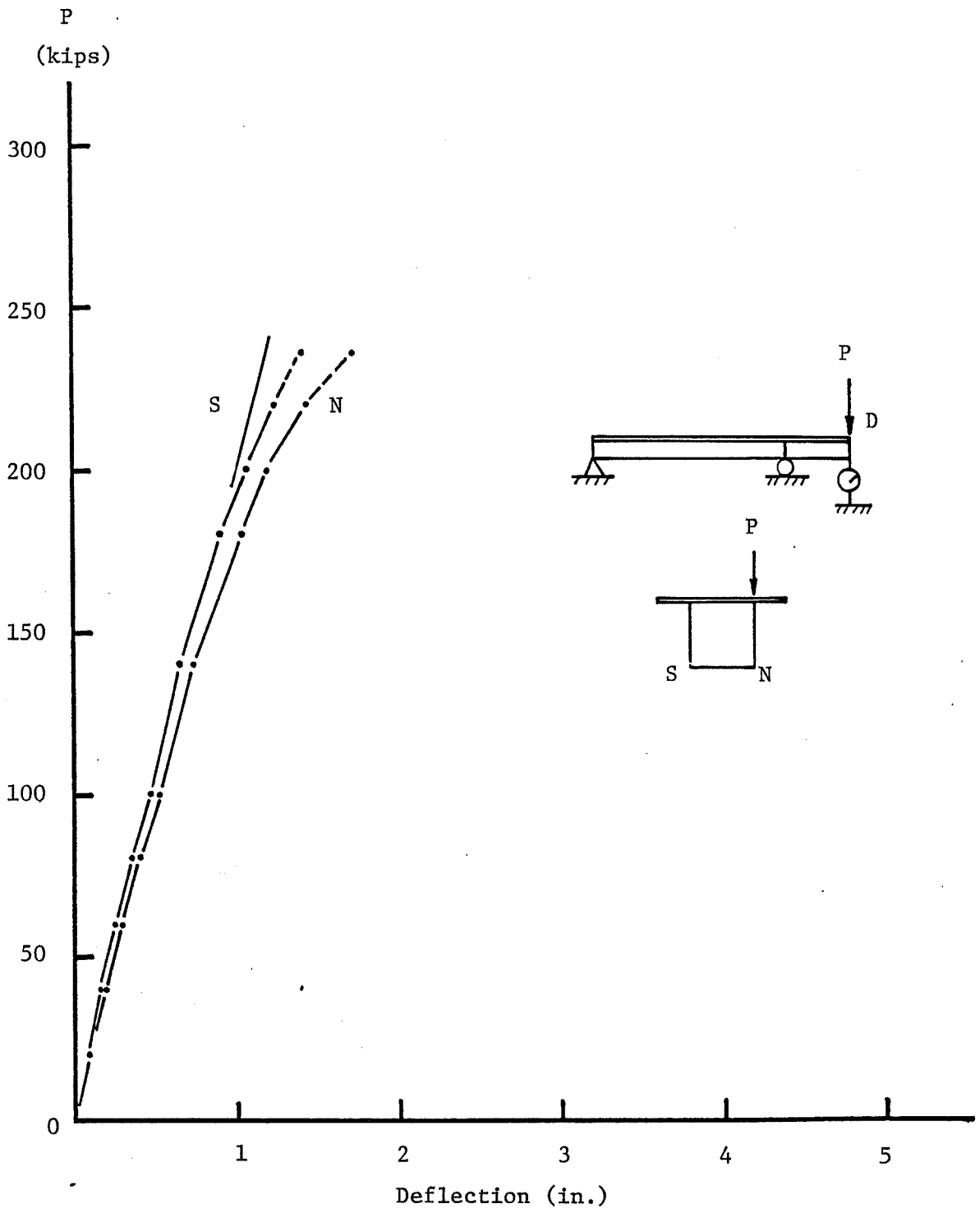

Fig. 5.6 Load-Deflection Diagrams, Test L1-CD

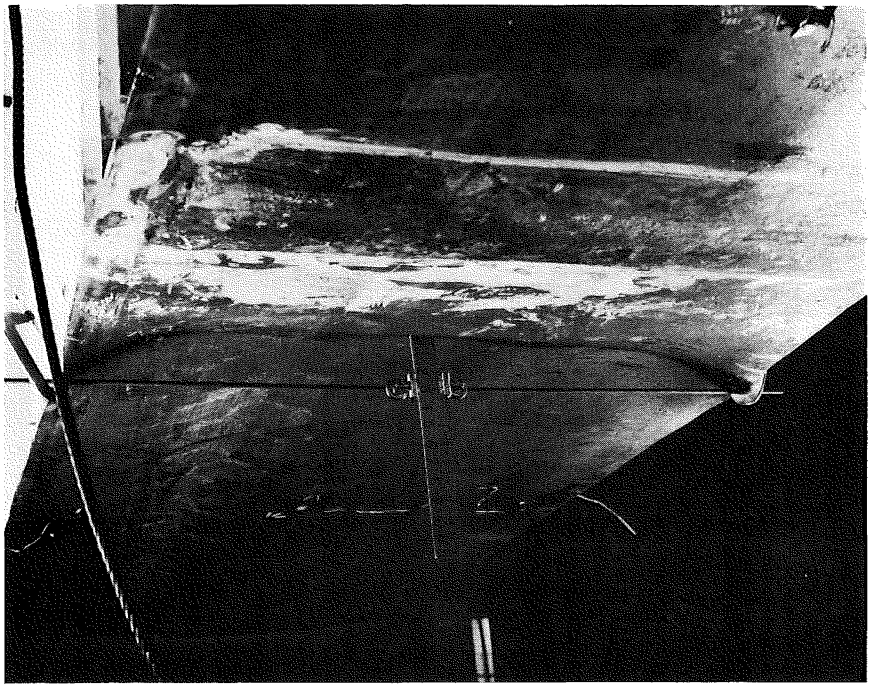

Fig. 5.7 Failed Compression Flange, Panel 12, L1-CD

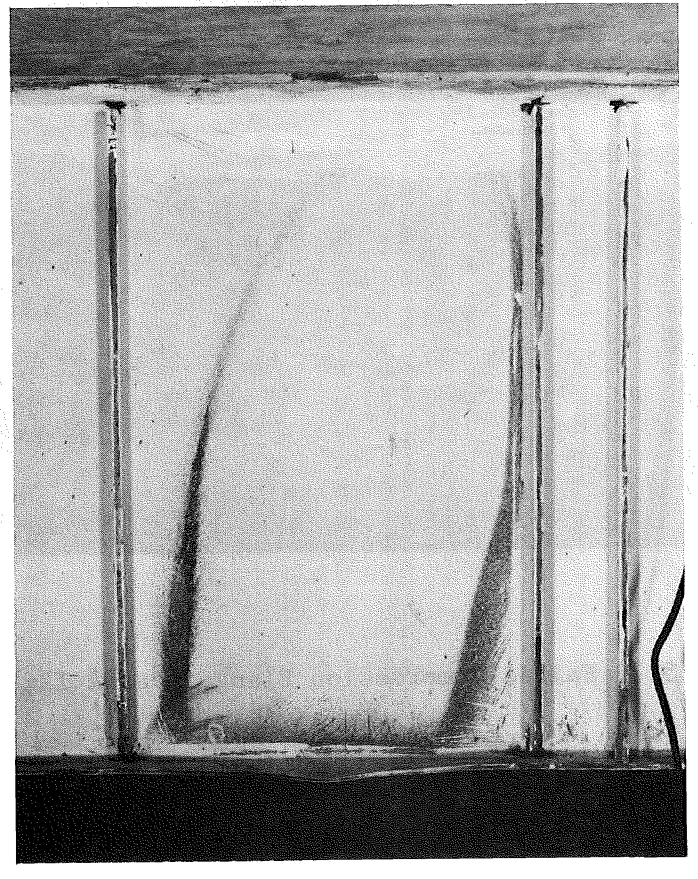

Fig. 5.8 Failed South Web, Panel 12, L1-CD

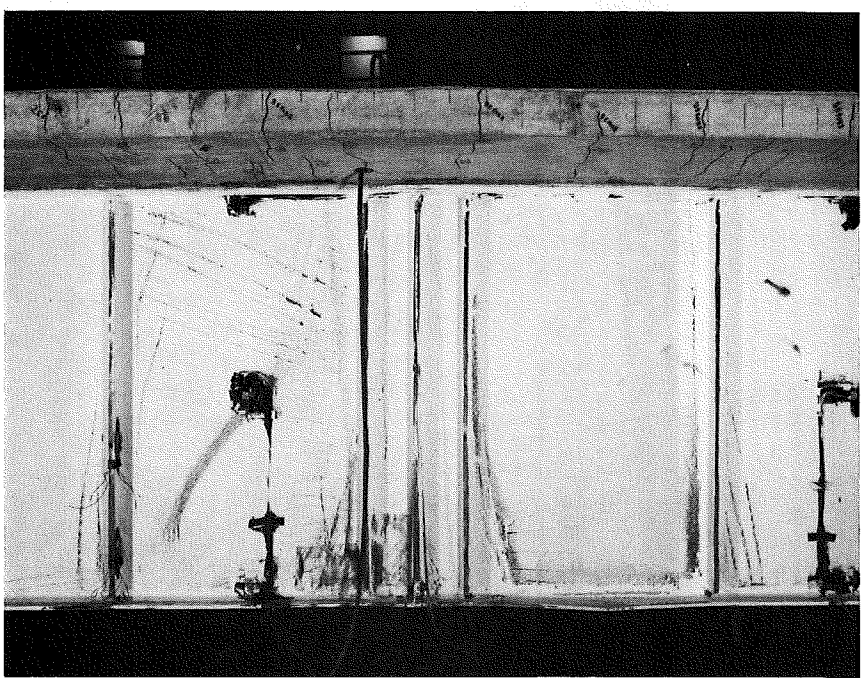

Fig. 5.9 Failed North Web of Panel 11 and Tension Field Diagonal in Panel 13, L1-CD

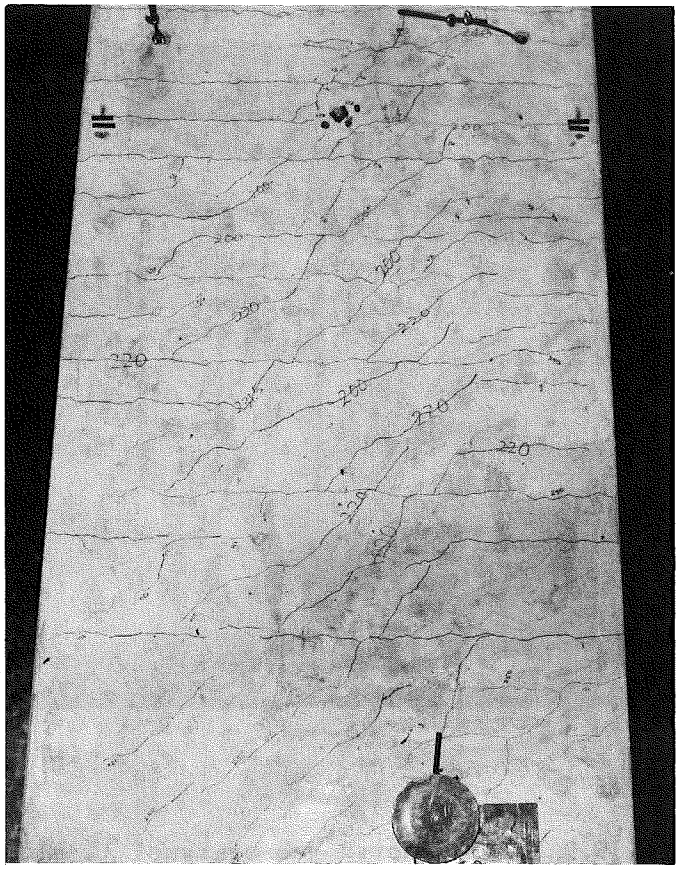

Fig. 5.10 Concrete Deck after Test L1-CD, Overhand Span

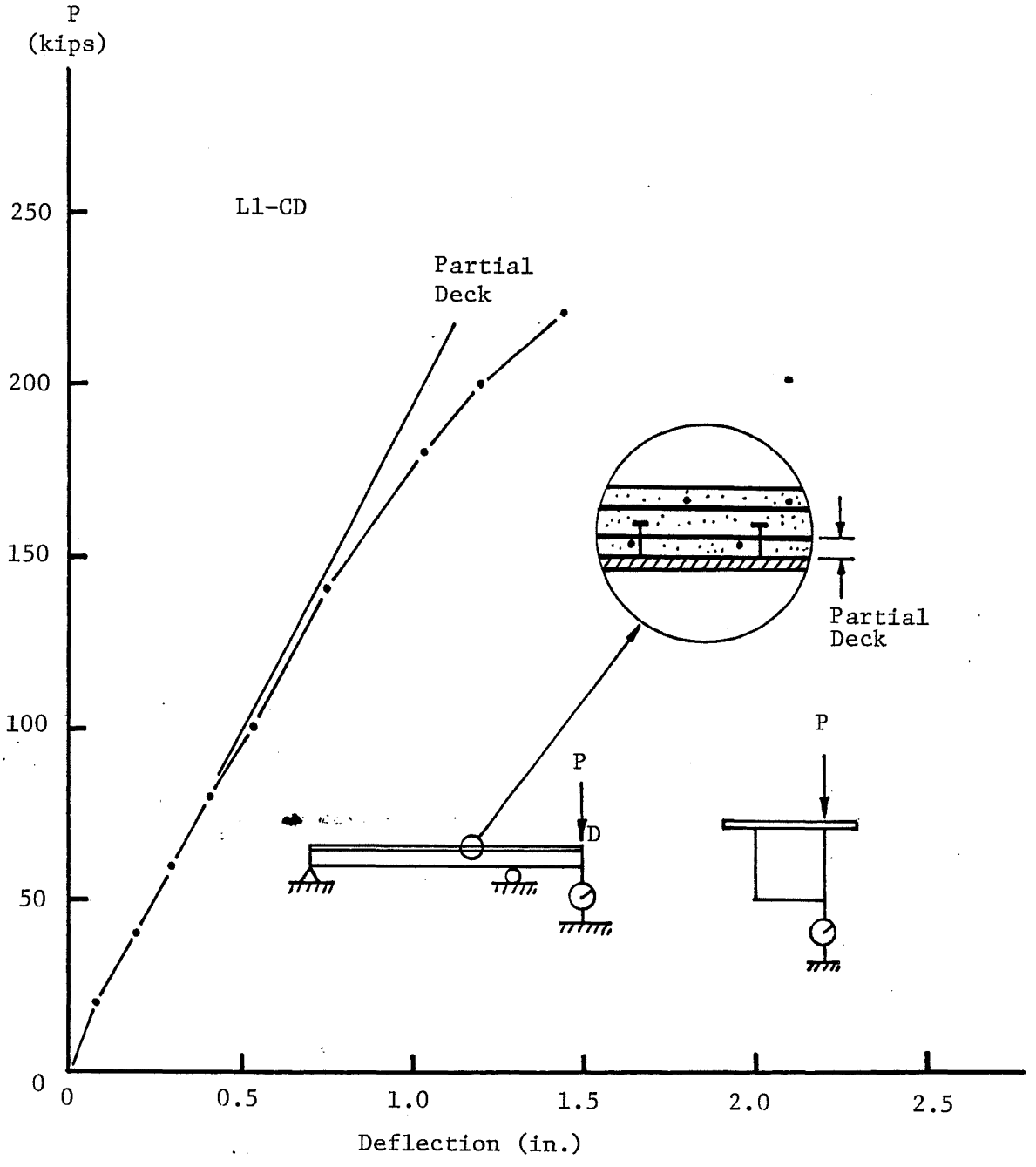

Fig. 5.11 Partial Deck Thickness for Negative Bending Moment

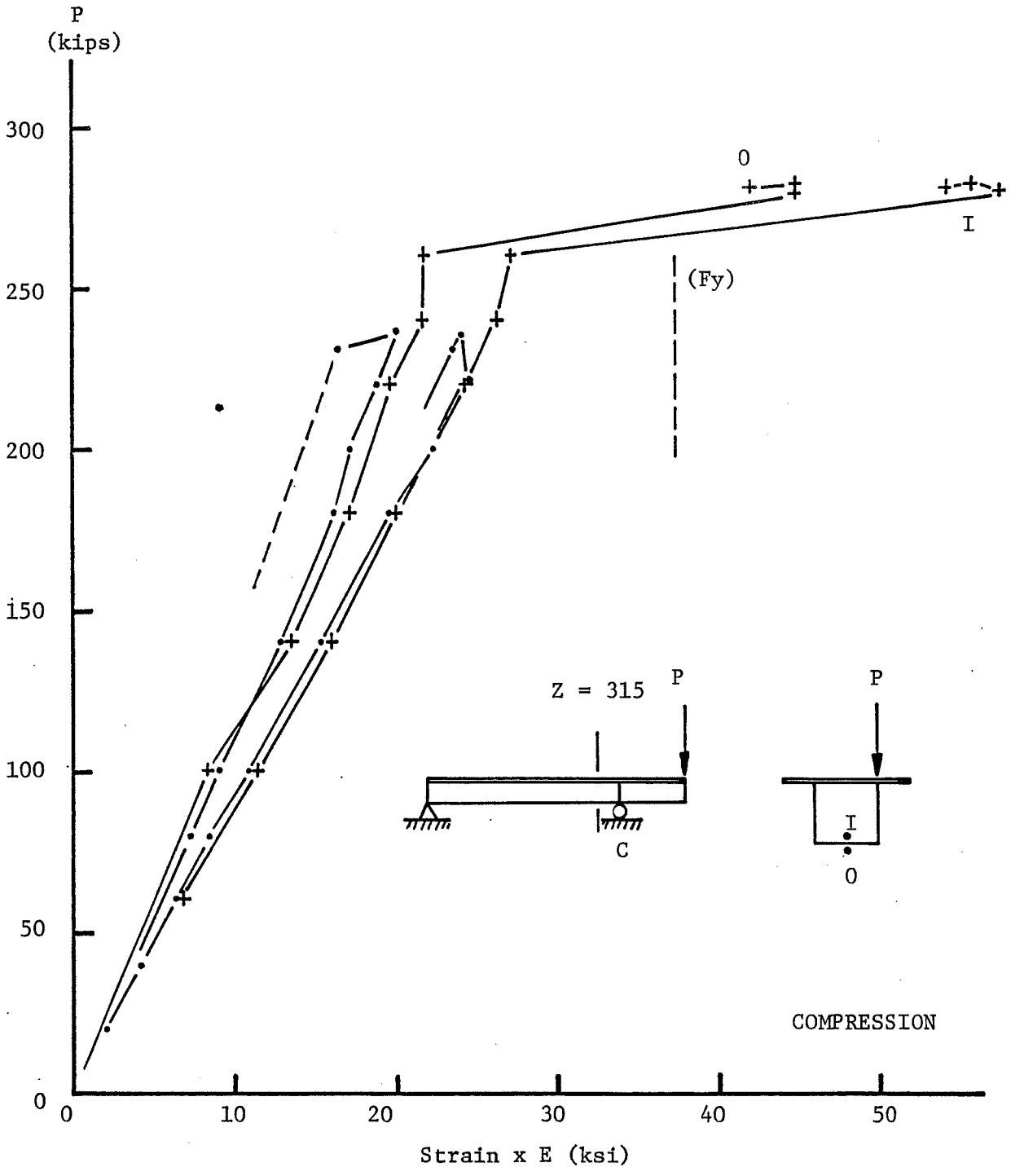

Fig. 5.12 Normal Strains on Surface of Compression Flange Plate, L1-CD

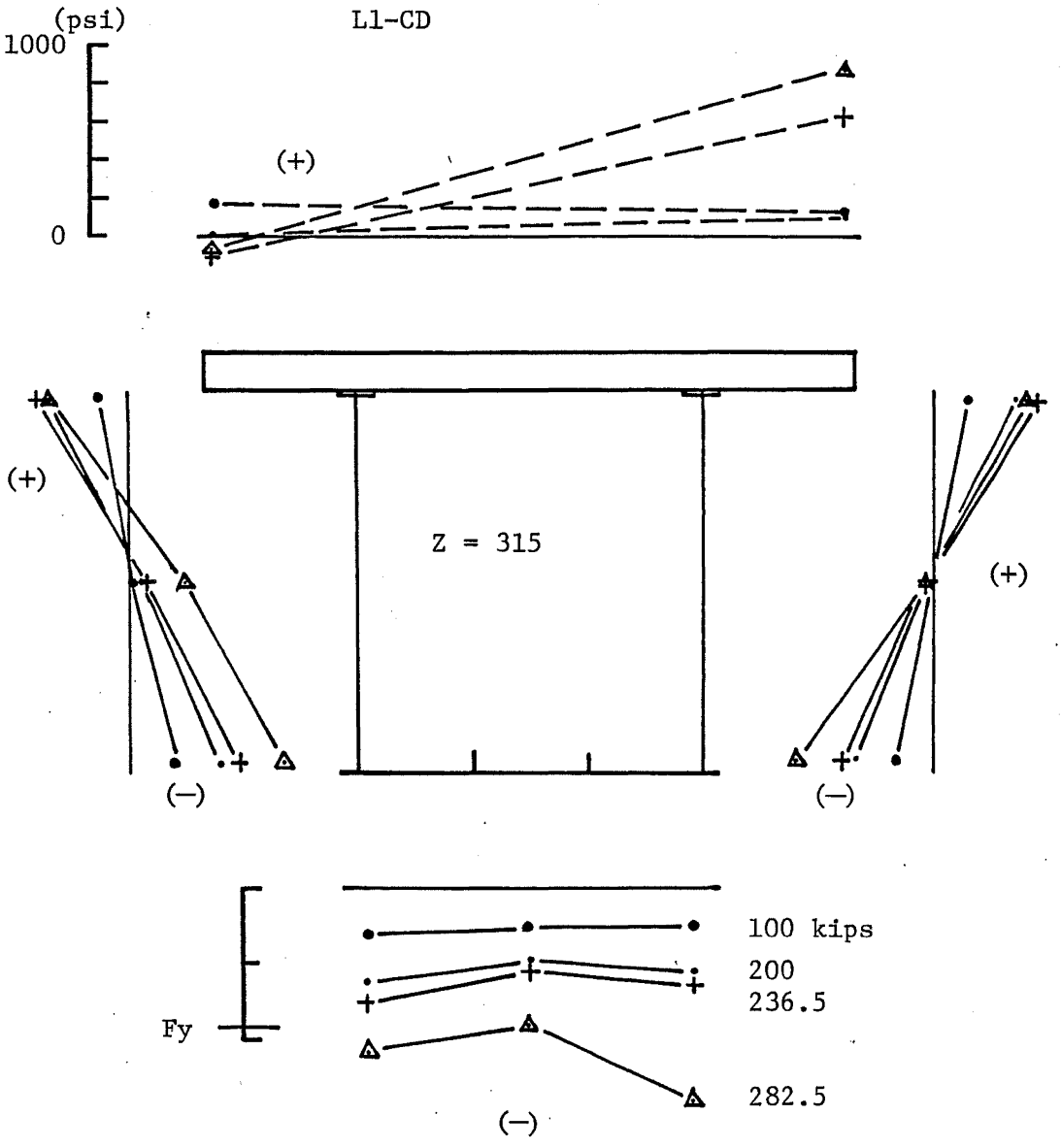

Fig. 5.13 Stress Distribution in Cross-section, Z = 315 in., L1-CD

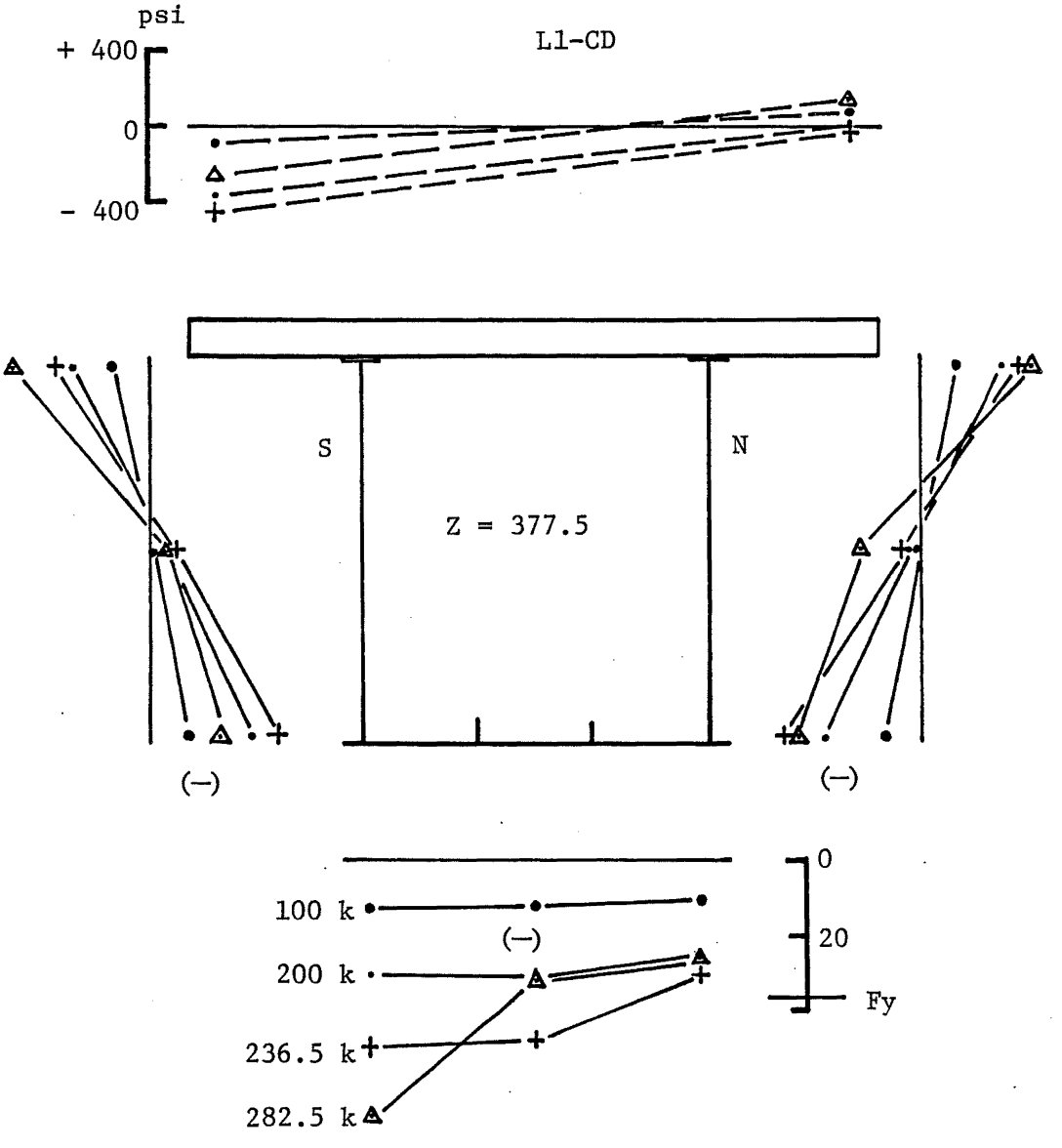

Fig. 5.14 Stress Distribution in Cross-section, Z = 377.5 in., L1-CD

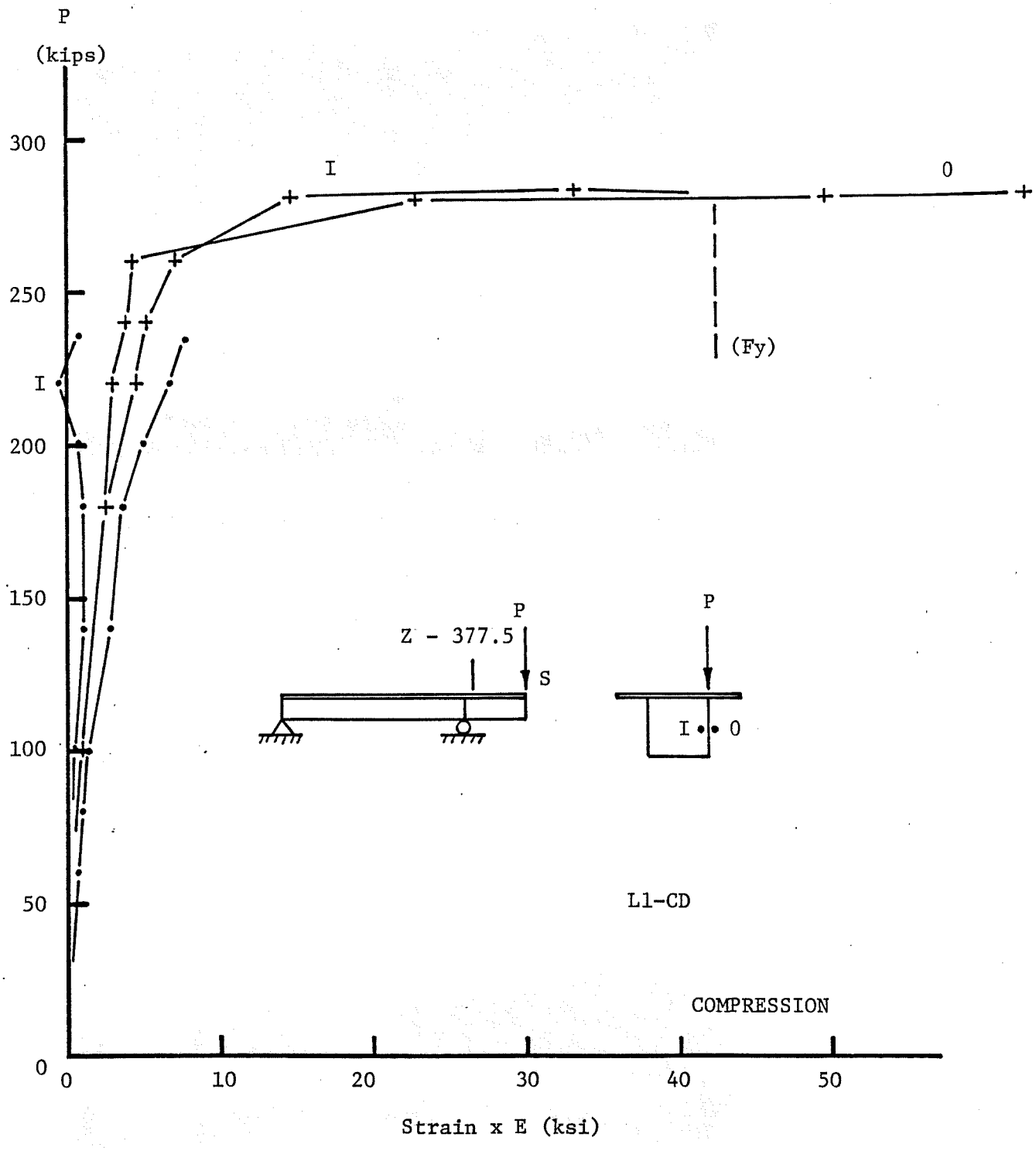

Fig. 5.15 Normal Strains on Surface of North Web, Z = 377.5 in., L1-CD

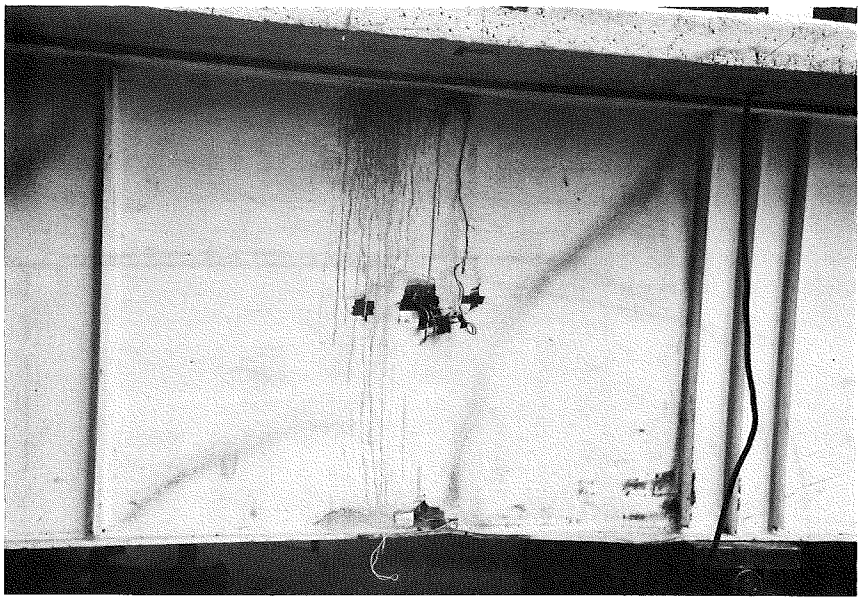

Fig. 5.16 North Web of Failed Box Panel 8, L2-CD

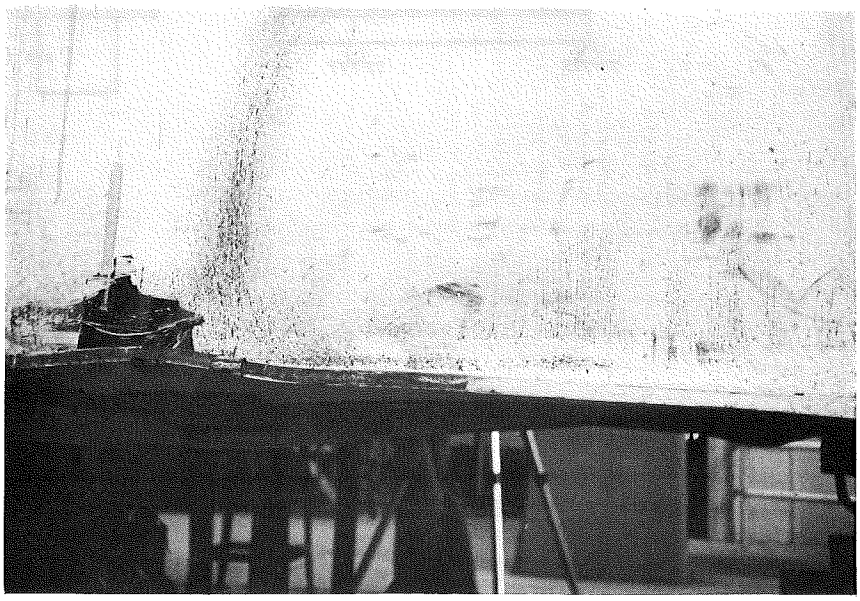

Fig. 5.17 Buckled Bottom Flange and Yielded Web, L2-CD

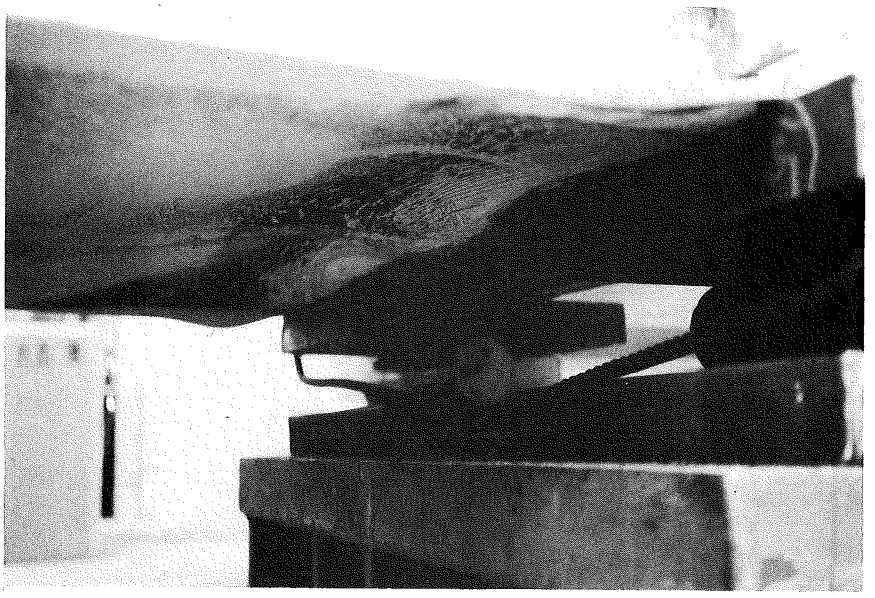

Fig. 5.18 Buckled Compression Flange at Support Test, L2-CD

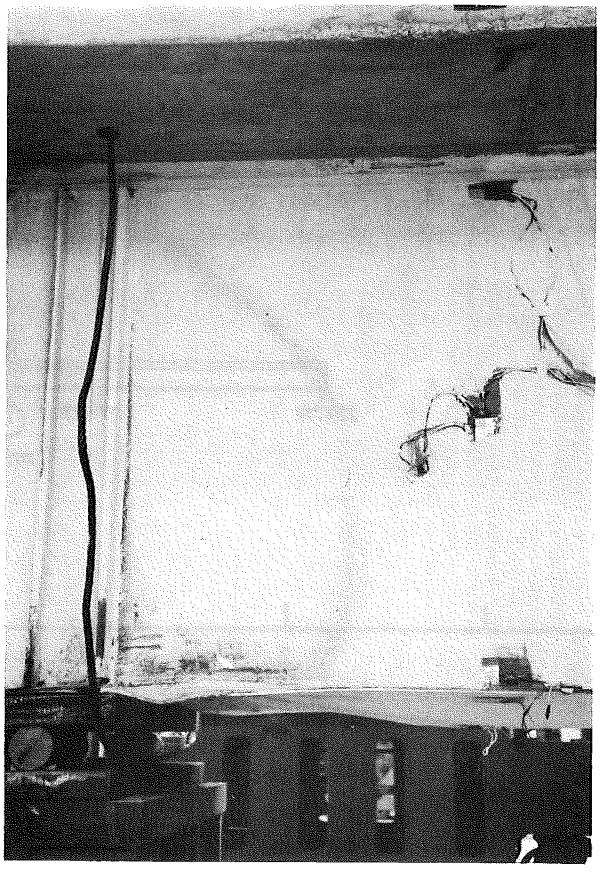

Fig. 5.19 Failure at Bottom Flange and South Web, L2-CD

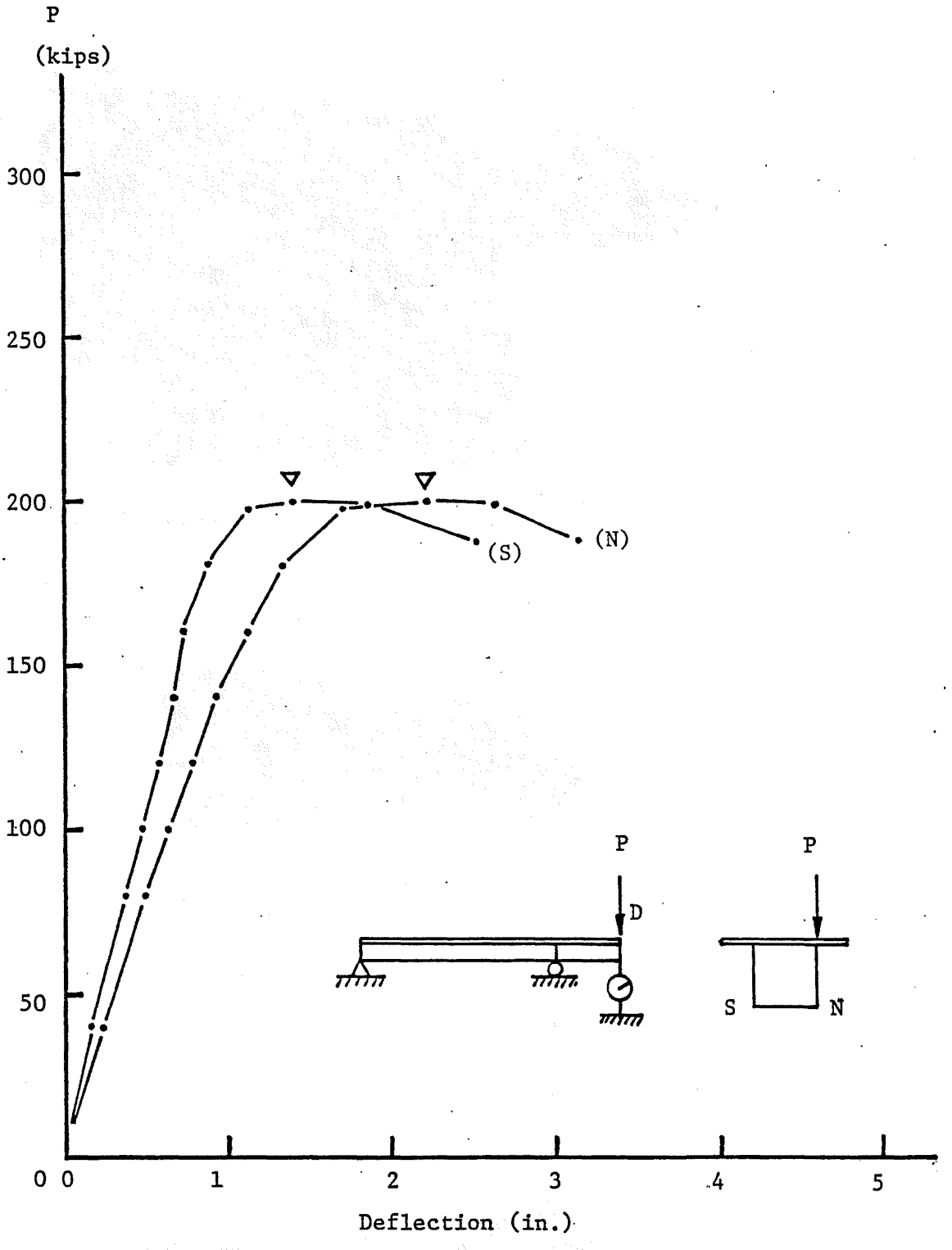

Fig. 5.20 Load-Deflection Diagram,- Test L2-CD

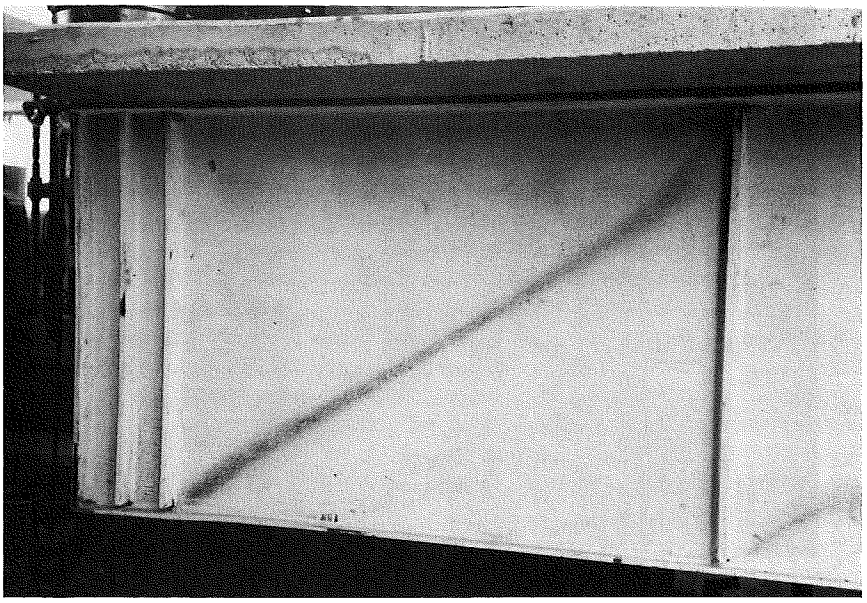

Fig. 5.21 Tension Field in North Web of End Panel, Test L2-CD

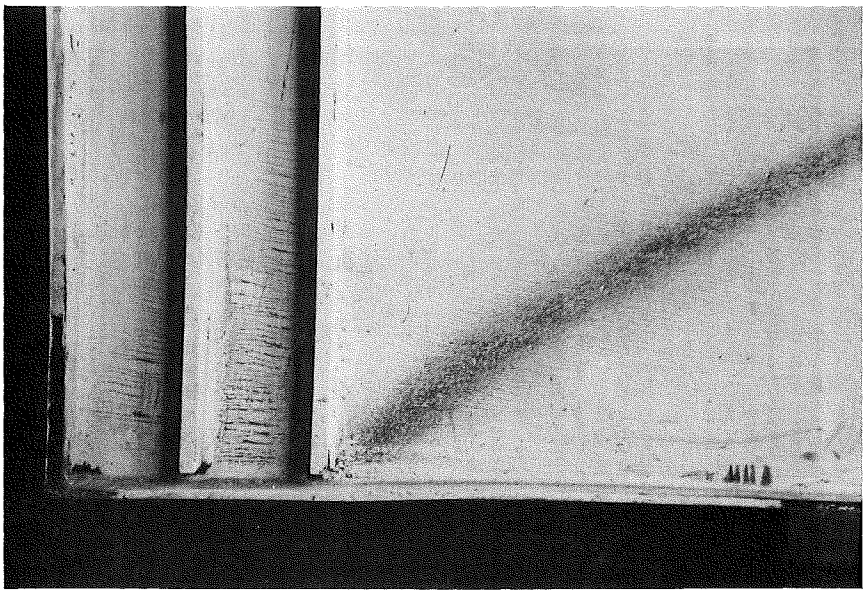

Fig. 5.22 Yielding at Stiffener and Bending of Bottom Flange End Panel, L2-CD

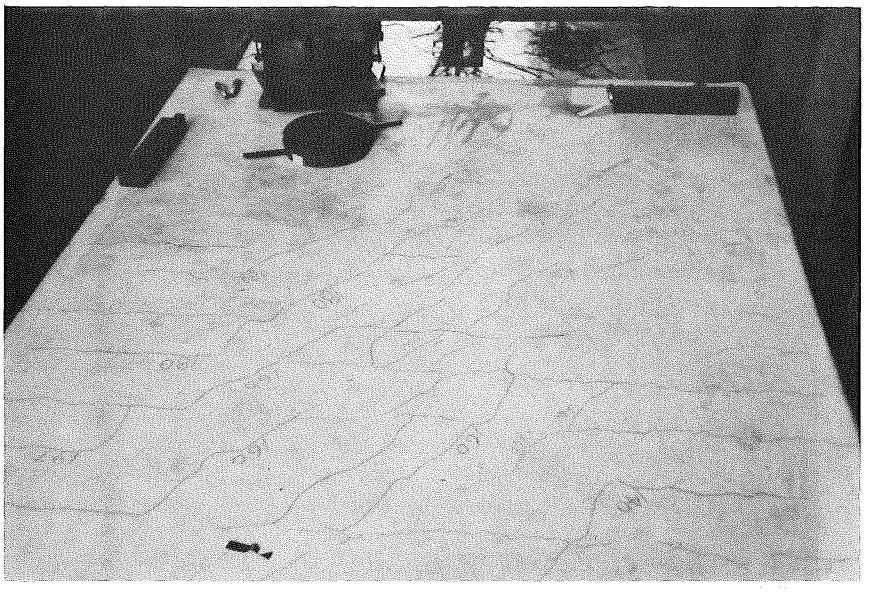

Fig. 5.23 Cracks on Concrete Deck Surface over End Panel, L2-CD

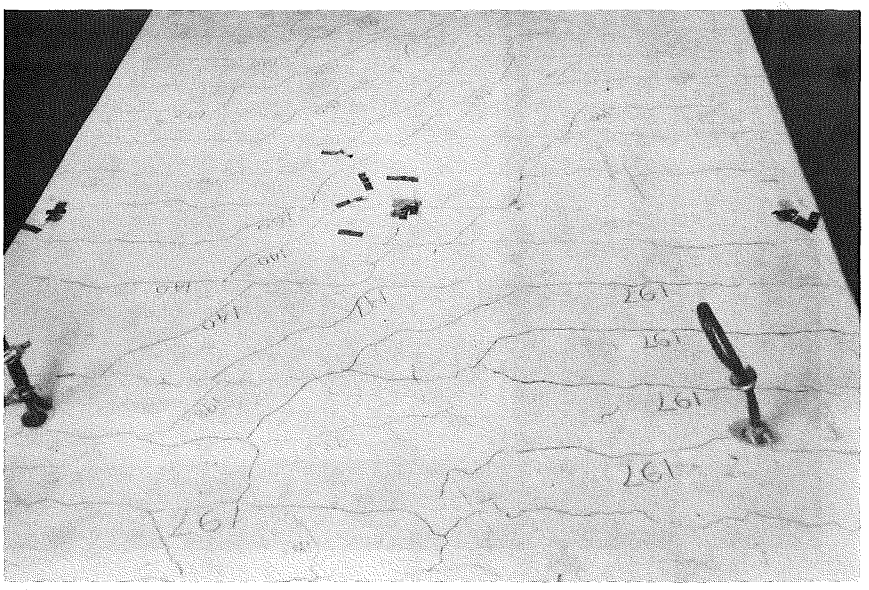

Fig. 5.24 Cracks on Concrete Deck Surface over Panel 8, L2-CD

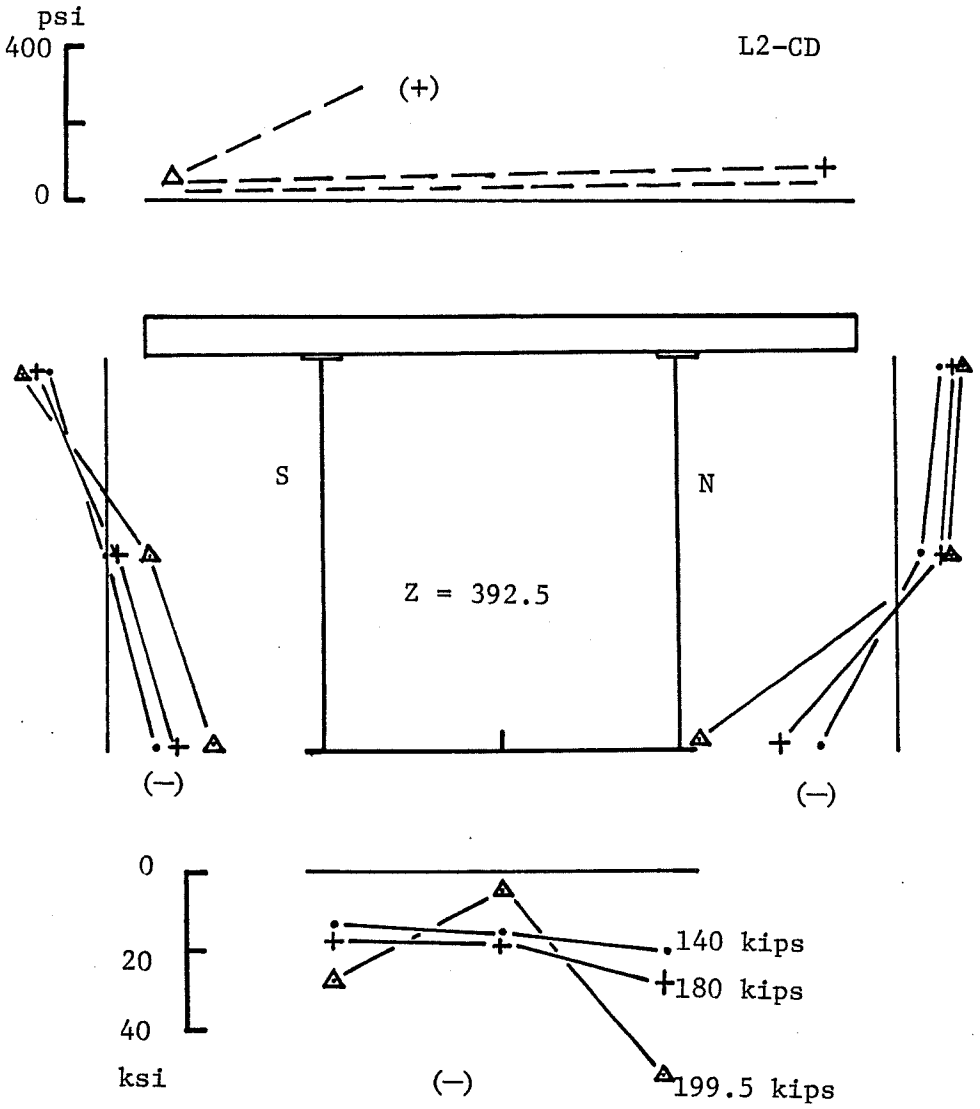

Fig. 5.25 Stress Distribution in Cross-section, Z = 392.5 in., L2-CD

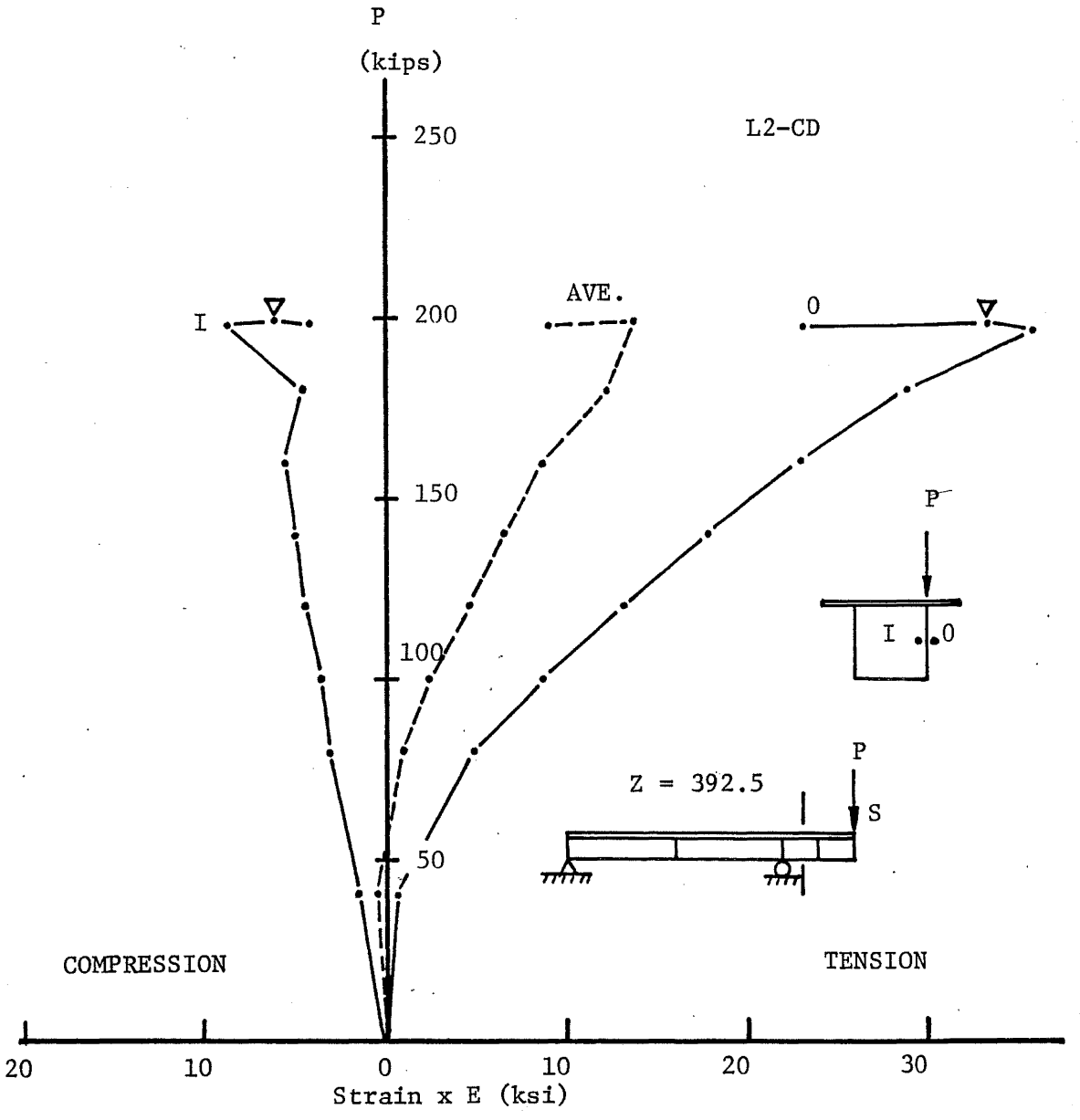

Fig. 5.26 Normal Strain on Surface of North Web, Z = 392.5 in., L2-CD

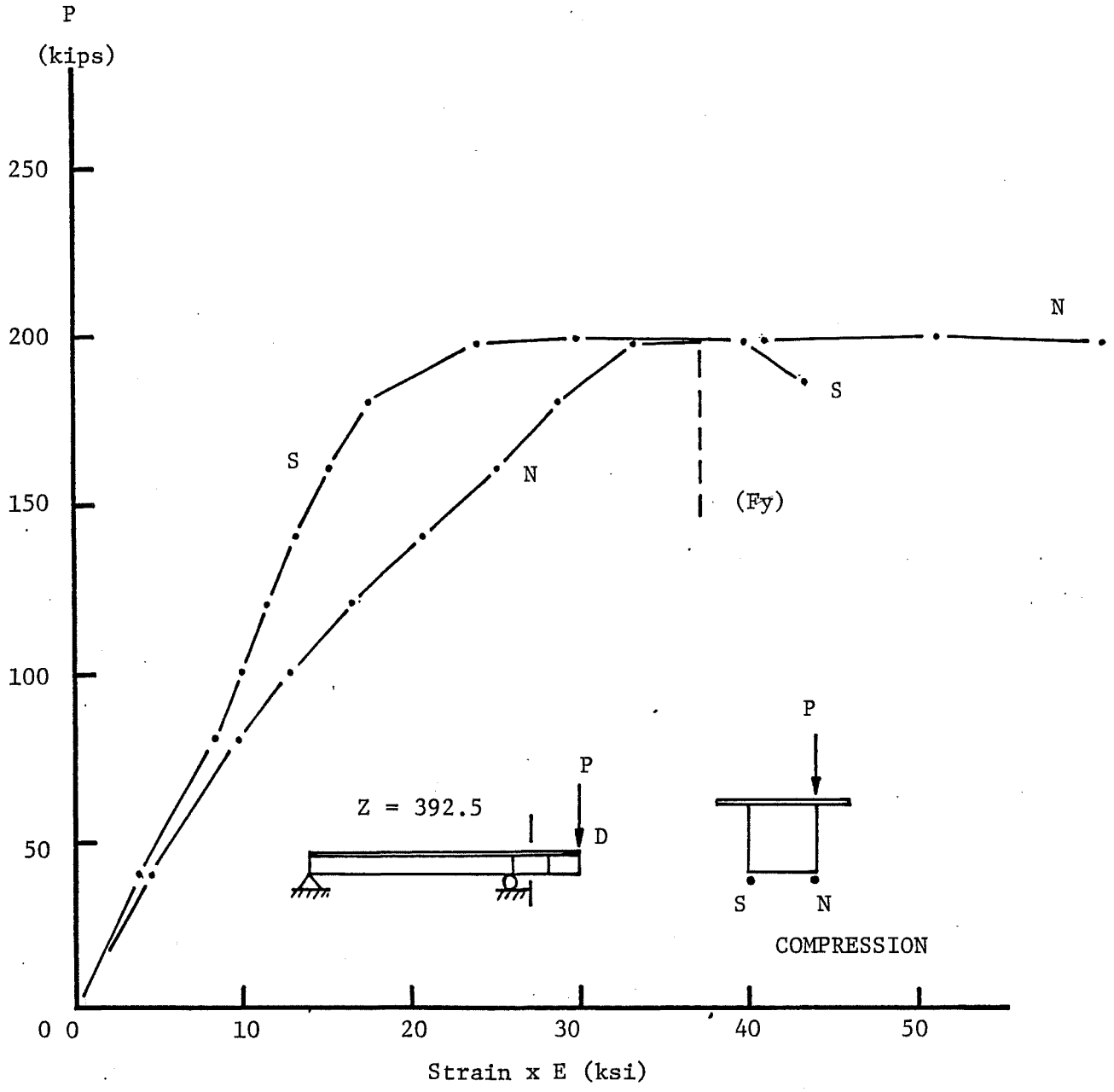

Fig. 5.27 Strains in Bottom Flange, Z = 392.5 in., L2-CD

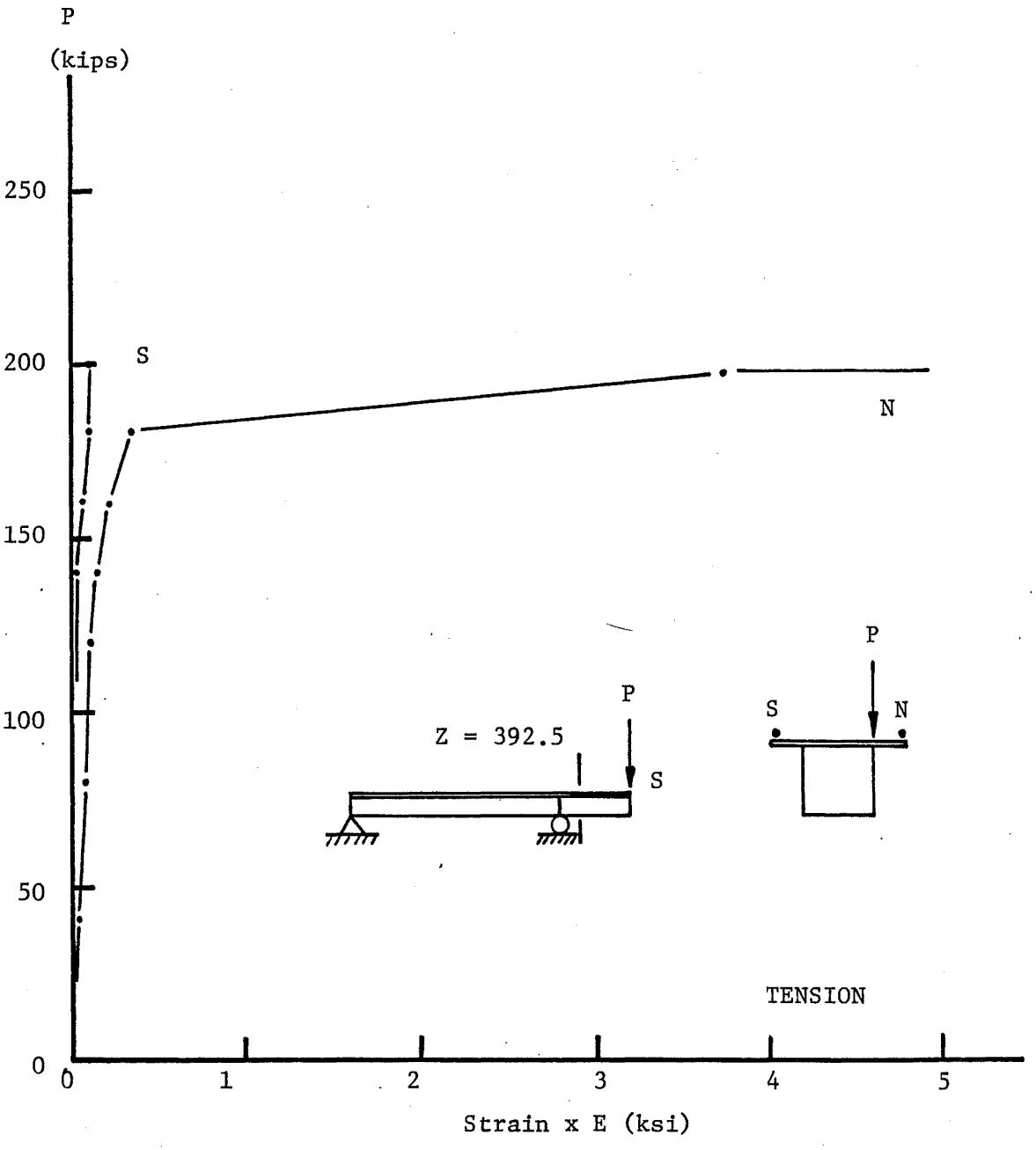

Fig. 5.28 Average Strains in Concrete Deck, Z = 392.5 in., L2-CD

REFERENCES

1.1 Subcommittee on Box Girder Bridges, ASCE-AASHTO Committee on Flexural Members
TRENDS IN THE DESIGN OF BOX GIRDER BRIDGES,
Journal of the Structural Division, ASCE, Vol. 93, No. ST3, Proc. Paper 5278, June 1967.

1.2 Subcommittee on Box Girder Bridges, ASCE-AASHTO Committee on Flexural Members
PROGRESS REPORT ON STEEL BOX GIRDER BRIDGES,
Journal of the Structural Division, ASCE, Vol. 97, No. ST4, Proc. Paper 8068, April 1971.

1.3 Petzold, E. H. and Galambos, T. V.
BEHAVIOR AND DESIGN OF LARGE STEEL BOX GIRDER BRIDGES,
Civil and Environmental Engineering Department Research Report No. 26, Washington University, St. Louis, MO, December 1973.

1.4 Basler, K.
STRENGTH OF PLATE GIRDERS IN SHEAR,
Journal of the Structural Division, Proc. of ASCE, Vol. 87, No. ST7, October 1961.

1.5 Chern, C. and Ostapenko, A.
ULTIMATE STRENGTH OF PLATE GIRDERS UNDER SHEAR,
Fritz Engineering Laboratory Report No. 328.7, Department of Civil Engineering, Lehigh University, August 1965.

1.6 Subcommittee on Ultimate Strength of Box Girders, ASCE-AASHTO Task Committee on Flexural Members,
STEEL BOX GIRDER BRIDGE ULTIMATE STRENGTH CONSIDERATIONS,
Journal of the Structural Division, ASCE, Vol. 100, No. ST12, Proc. Paper 11014, December 1974.

1.7 The Merison Committee
INQUIRY INTO THE BASIS OF DESIGN AND METHOD OF ERECTION OF STEEL BOX GIRDER BRIDGES, Report of the Committee, Appendix 1, Interim Design and Workmanship Rules, Department of Environment, Scottish Development Department, Welsh Office, February 1973.

1.8 Chen, Y. S. and Yen, B.T.
ANALYSIS OF COMPOSITE BOX GIRDERS,
Fritz Engineering Laboratory Report No. 380.12,
Department of Civil Engineering, Lehigh University,
April 1980.

1.9 Chen, Y. S.
ULTIMATE STRENGTH OF RECTANGULAR COMPOSITE BOX GIRDERS,
Ph.D. Dissertation, Department of Civil Engineering,
Lehigh University, Bethlehem, Pennsylvania, December
1976.

1.10 Chen, Y. S. and Yen, B. T.
ULTIMATE STRENGTH OF COMPOSITE BOX GIRDERS IN FLEXURE,
Fritz Engineering Laboratory Report No. 380.15,
Department of Civil Engineering, Lehigh University,
April 1980.

2.1 American Association of State Highway and Transportation Officials,
STANDARD SPECIFICATIONS FOR HIGHWAY BRIDGES,
Eleventh Edition, 1973.

2.2 Tall, L. et al
STRUCTURAL STEEL DESIGN, Second Edition, Ronald Press,
New York, 1974.

2.3 Galambos, T. V.
STRUCTURAL MEMBERS AND FRAMES,
Prentice Hall, Inc., Englewood Cliffs, New Jersey, 1968.

2.4 Vlasov, V. Z.
THIN-WALLED ELASTIC BEAMS,
The Israel Program for Scientific Translation,
Jerusaleum, 1961; Available from the Office of Technical
Service, U. S. Department of Commerce, Washington, D. C.

3.1 Kollbrunner, C. F. and Basler, K.
TORSION IN STRUCTURES, Springer-Verlag, New York, 1969.

3.2 McDonald, R. E., Chen, Y. S., Yilmaz, C. and Yen, B. T.
ANALYSIS OF OPEN STEEL BOX SECTIONS WITH BRACING,
Journal of the Structural Division, ASCE, Vol. 102, No.
ST1, Proc. Paper 11850, January 1976.

REFERENCES (continued)

4.1 Corrado, J. A. and Yen, B. T.
FAILURE TESTS OF RECTANGULAR MODEL STEEL BOX GIRDERS, Journal of the Structural Division, ASCE, Vol. 99, No. ST7, Proc. Paper 9854, July 1973.

4.2 Corrado, J. A.
ULTIMATE STRENGTH OF SINGLE SPAN RECTANGULAR STEEL BOX GIRDERS, Ph.D. Dissertation, Department of Civil Engineering, Lehigh University, Bethlehem, Pennsylvania.

4.3 Basler, K., Yen, B. T., Mueller, J. A. and Thurliman, B.
WEB BUCKLING TESTS ON WELDED PLATE GIRDERS, Bulletin No. 64, Welding Research Council, New York, September 1960.

4.4 Slutter, R. G. and Driscoll, G. C.
ULTIMATE STRENGTH OF COMPOSITE MEMBERS, ASCE, Conference on Composite Design in Steel and Concrete for Bridge and Building, Pittsburgh, Pennsylvania, 1962.